LMSC-F277133
December 23, 1988

(4)

# MAGNETIC RESONANCE IMAGING STUDIES OF PROCESS RHEOLOGY

Research supported by the SDIO Innovative Science and Technology Office and managed by the Office of Naval Research



G.A. Lo
J.C. Crowley
S.W. Sinton
D.T. Wadiak
R. van de Griend

Lockheed Missiles and Space Co., Inc.
Lockheed Palo Alto Research Laboratory
3521 Hanover Street, O/93-50, B/204
Palo Alto, CA 94304

A.B. Kunz
M.J. Seel
S.A. Marshall
B.H. Suits

Michigan Technological University
Department of Physics
Houghton, MI 49931

23 December 1988

Technical Report for Period: 1 Oct 1986 to 31 July 1988
Contract Number N00014-86-C-0724

Prepared for
STRATEGIC DEFENSE INITIATIVE ORGANIZATION
Innovative Science and Technology Office
Washington, DC 20301-7100

OFFICE OF NAVAL RESEARCH
800 North Quincy Street
Arlington, VA 22217-5000

UNCLASSIFIED
SECURITY CLASSIFICATION OF THIS PAGE

# REPORT DOCUMENTATION PAGE

Form Approved OMB No. 0704-0188

| | |
|---|---|
| 1a. REPORT SECURITY CLASSIFICATION: Unclassified | 1b. RESTRICTIVE MARKINGS |
| 2a. SECURITY CLASSIFICATION AUTHORITY | 3. DISTRIBUTION/AVAILABILITY OF REPORT: Unclassified. Distribution Unlimited |
| 2b. DECLASSIFICATION/DOWNGRADING SCHEDULE | |
| 4. PERFORMING ORGANIZATION REPORT NUMBER(S): LMSC F277133 | 5. MONITORING ORGANIZATION REPORT NUMBER(S) |
| 6a. NAME OF PERFORMING ORGANIZATION: Lockheed Missiles & Space Co. Research & Development Divis. / 6b. OFFICE SYMBOL (If applicable): 0/93-50 | 7a. NAME OF MONITORING ORGANIZATION: Office of Naval Research |
| 6c. ADDRESS (City, State, and ZIP Code): 3251 Hanover Street, Palo Alto, CA 94304 | 7b. ADDRESS (City, State, and ZIP Code): 800 North Quincy Street #619, Arlington, VA 22217-5000 |
| 8a. NAME OF FUNDING/SPONSORING ORGANIZATION: Strategic Defense Initiative Organization Innovative Science & Tech Office / 8b. OFFICE SYMBOL (If applicable): SDIO/IST | 9. PROCUREMENT INSTRUMENT IDENTIFICATION NUMBER: N00014-86-C-0724 |
| 8c. ADDRESS (City, State, and ZIP Code): Washington, DC 20301-7100 | 10. SOURCE OF FUNDING NUMBERS: PROGRAM ELEMENT NO. 63222C; PROJECT NO. 2400; TASK NO.; WORK UNIT ACCESSION NO NR-Z400015-SR501 |

11. TITLE (Include Security Classification)
Magnetic Resonance Studies of Process Rheology (U)

12. PERSONAL AUTHOR(S)
Crowley, Joseph C.; Sinton, Steven W.; Wadiak, David T.; van de Griend, Renée; Lo, George A.

| 13a. TYPE OF REPORT | 13b. TIME COVERED | 14. DATE OF REPORT (Year, Month, Day) | 15. PAGE COUNT |
|---|---|---|---|
| Interim | FROM Oct 86 TO July 88 | 1988 December 23 | 55 |

16. SUPPLEMENTARY NOTATION Prepared in cooperation with Michigan Technological University Dept. of Physics: Kunz, A. Barry; Seel, Max; Suits, Bryan H.; Marshall, Sam A.

| 17. COSATI CODES | | | 18. SUBJECT TERMS (Continue on reverse if necessary and identify by block number) |
|---|---|---|---|
| FIELD | GROUP | SUB-GROUP | Propellants, Continuous Processing, NMR, ESR, MRI, Quantum Mechanics, Stokesian Dynamics, Rheology |
| | | | |
| | | | |

19. ABSTRACT (Continue on reverse if necessary and identify by block number)


The objective of this program is to develop magnetic resonance imaging and numerical modeling methods which will provide for improved methods of flow analysis as well as an improved understanding of the flow behavior of solid-particle-filled polymeric suspensions such as uncured solid rocket propellant.

This program has designed and evaluated a simplified flow system for initial evaluation of Nuclear Magnetic Resonance (NMR) flow imaging methods (as applied to viscous solid-filed suspensions) and has ordered a pilot-plant scale (50 mm diameter) flow system for use in the coming year. By applying state-of-the-art multiple pulse techniques, this program obtained the first-ever NMR image of solid


| | |
|---|---|
| 20. DISTRIBUTION/AVAILABILITY OF ABSTRACT: ☒ UNCLASSIFIED/UNLIMITED ☐ SAME AS RPT ☐ DTIC USERS | 21. ABSTRACT SECURITY CLASSIFICATION: Unclassified |
| 22a. NAME OF RESPONSIBLE INDIVIDUAL: Dr. R.S. Miller | 22b. TELEPHONE (Include Area Code): (202) 696-4403 / 22c. OFFICE SYMBOL: Code 1132P |

DD Form 1473, JUN 86 *Previous editions are obsolete.* SECURITY CLASSIFICATION OF THIS PAGE

Unclassified

aluminum particles in cured solid propellant simulant. This program obtained NMR images of the polymer component of both cured and uncured propellant simulants. These images showed clearly that concentration inhomogeneities, voids, and defects (cracks) are readily detectable. The current resolution in NMR images of the polymer (binder / plasticizer) components of modern, high-energy, highly plasticized propellant simulants was found to be on the order of 100 μm. The degree of homogeneity observed in NMR images of the plasticizer/binder in these samples correlated with their known processing history.

A continuous-wave electron spin resonance spectrometer at Michigan Technological University was configured for imaging, and initial studies were carried out to determine the potential of the technique for propellant analysis. The spectrometer was then modified to a low-power pulse-echo configuration and initial studies of this setup were carried out.

Preliminary numerical modeling studies were carried out using the quantum mechanical (QM) and Stokesian Dynamics (SD) models in an uncoupled mode. The initial QM analyses of particle-filled polymeric suspensions yielded reasonable intramolecular polymer-polymer forces, and polymer-particle interaction forces. The attractive Van der Waals potential between polymer units was determined, along with the chain slip barrier. The SD model was also run in an uncoupled mode, and was used to predict how various flow conditions would affect the evolution of structure in a suspension. The two models (QM and SD) were then linked together. In this mode, particle-particle interactions, as calculated by the QM model are allowed to influence the evolution of the overall suspension system, as calculated by the SD model. To couple the models, a linearized Lennard-Jones particle-particle attractive force was added to the SD model. Phenomena such as the tendency of particles to agglomerate or cluster could be affected by this force. This may be of particular interest in propellant systems because, in propellants, the fine particles often dominate the population. Preliminary results of the coupled model are presented in this report.

## TABLE OF CONTENTS


| Section | | Page |
|---|---|---|
| **LIST OF FIGURES** | | ii |
| **LIST OF ABBREVIATIONS** | | iii |
| **1.** | **INTRODUCTION** | 1 |
| 1.1 | BACKGROUND | 1 |
| 1.2 | OBJECTIVES | 1 |
| 1.3 | PROGRESS SUMMARY | 2 |
| 1.4 | SUMMARY OF PLANS AND PROJECTED PROGRESS | 4 |
| **2.** | **PROGRAM STATUS** | 6 |
| 2.1 | Rheological Studies | 6 |
| 2.2 | Nuclear Magnetic Resonance Studies | 9 |
| 2.2.1 | LPARL. | 9 |
| 2.2.2 | MTU. | 13 |
| 2.3 | Electron Spin Resonance Studies | 15 |
| 2.4 | Image Processing | 15 |
| 2.5 | Theoretical Modeling | 16 |
| 2.5.1 | Quantum Mechanics. | 17 |
| 2.5.2 | Stokesian Dynamics Modeling. | 18 |
| 2.5.3 | Coupled QM/SD Model. | 18 |
| **3.** | **PROGRAM PLANS** | 23 |
| 3.1 | Rheological Studies | 23 |
| 3.2 | Nuclear Magnetic Resonance Studies | 23 |
| 3.2.1 | NMR Spectroscopy / Imaging of Fluids. | 24 |
| 3.2.2 | NMR Spectroscopy / Imaging of Particles. | 24 |
| 3.2.3 | NMR Spectroscopy Probe Gradient Accessory. | 25 |
| 3.2.4 | Processing of Velocity/Positional-Encoded Images. | 25 |
| 3.3 | Electron Spin Resonance Studies | 25 |
| 3.4 | Image Processing | 26 |
| 3.5 | Theoretical Modeling | 26 |
| 3.5.1 | QM and SD Models. | 26 |
| 3.5.2 | Finite Element Flow Dynamics Modeling. | 27 |
| **4.** | **COLLABORATIONS WITH OTHER PROGRAMS** | 29 |
| 4.1 | Massachusetts Institute of Technology | 29 |
| **5.** | **SCHEDULE** | 31 |

Attachments:

A. Revised Program Schedule Plan for 1988 to Early 1989..... A-1

## LIST OF FIGURES


| Figure | | Page |
|---|---|---|
| Figure 1: | Rheometrics RMS-800 Mechanical Spectrometer (a) complete instrument, (b) test station with parallel-plate fixture installed. | 32 |
| Figure 2: | Schematic diagram of MRI flow system | 33 |
| Figure 3: | Zero shear rate viscosity results for suspensions of glass spheres in 120 poise corn syrup | 34 |
| Figure 4: | Torque output of step shear reversal tests for suspensions of 10 μm glass spheres and corn syrup | 34 |
| Figure 5: | NMR images of H-nuclei in four PBAN simulant samples. Mixing time of samples increases as A → B → C → D | 35 |
| Figure 6: | Histogram plots of pixel intensity for each of the four PBAN images (images shown in Figure 5). As mixing time increases (A → B → C → D), separation of signal and noise peaks increases, and width of signal peak decreases. | 36 |
| Figure 7: | NMR images of hydrogen nuclei in pure glycerine (left) and a suspension of carbon-black in glycerine (right) | 37 |
| Figure 8: | Histogram plots for NMR images of pure glycerine and glycerine/carbon-black suspension (images shown in Figure 7) | 38 |
| Figure 9: | Hydrogen density plot for selected rows and columns in pure glycerine and glycerine / carbon-black NMR images (images shown in Figure 7) | 39 |
| Figure 10: | One-dimensional autocorrelation results for selected rows and columns of pure glycerine and glycerine/carbon-black NMR images (images shown in Figure 7) | 40 |
| Figure 11: | Autocorrelation results for selected columns of PBAN images (images shown in Figure 5) | 41 |
| Figure 12: | Autocorrelation results for selected rows of PBAN images (images shown in Figure 5) | 42 |
| Figure 13: | $^{23}$Na NMR image of PBAN-based propellant simulant sample (15mm x 9mm x 1mm) with hole (9mm x 2.5mm), obtained using initial MTU gradient coil design. Resolution ~3mm. | 43 |
| Figure 14: | $^{23}$Na NMR image of PBAN-based propellant simulant sample (15mm x 9mm x 1mm) with hole (9mm x 2.5mm), obtained using improved MTU gradient coil design. Resolution ~1mm. | 43 |
| Figure 15: | Illustration of Polyoxymethylene-polyoxymethylene interaction | 44 |
| Figure 16: | Polyoxymethylene-ammonium perchlorate interaction | 45 |
| Figure 17: | Illustration of Polyoxymethylene-aluminum interaction | 46 |
| Figure 18: | Illustration of model types and length scales | 47 |
| Figure 19: | Illustration of Lennard-Jones (L-J) and lubrication forces as a function of particle separation distance | 48 |
| Figure 20: | Plots of the inter-particle distance versus time for the two-particle simulation, with and without L-J (van der Waals, or vdW) forces. Basis of the two-particle simulation is illustrated in the figure inset. | 49 |
| Figure 21: | Plots of the relative L-J forces acting on the particles in the two-particle simulation | 50 |

## LIST OF ABBREVIATIONS

| | |
|---|---|
| 1-D | One-dimensional |
| 2-D | Two-dimensional |
| 3-D | Three-dimensional |
| AP | Ammonium Perchlorate |
| DPPH | 1,1'-DiPhenyl-2-PicrylHydrazyl |
| EM | Electromagnetic field |
| ESR | Electron Spin Resonance |
| FE | Finite Element |
| IF | Intermediate Frequency |
| IP | Image Processing |
| LMSC | Lockheed Missiles and Space Co., Inc. |
| LPARL | Lockheed Palo Alto Research Laboratory |
| MR | Magnetic Resonance |
| MRI | Magnetic Resonance Imaging |
| MTU | Michigan Technological University |
| NG | Nitroglycerine |
| NMR | Nuclear Magnetic Resonance |
| NOS/IH | Naval Ordnance Station at Indian Head, Maryland |
| ONR | Office of Naval Research |
| PBAN | Polybutadiene acrylonitrile |
| PEG | PolyEthylene Glycol |
| PIB | Polyisobutylene |
| POM | PolyOxyMethylene |
| QM | Quantum Mechanics |
| RF | Radiofrequency |
| SD | Stokesian Dynamics |
| SIT | Stevens Institute of Technology |
| TPV | TriPhenyl-Verdazyl |

# 1. INTRODUCTION

This report summarizes progress made to date on the following contract, hereafter referred to as the Program. This research is sponsored by the Innovative Science and Technology Office of the Strategic Defense Initiative Organization, and managed by the Office of Naval Research (ONR). The Program is a joint effort between the Lockheed Palo Alto Research Laboratory (LPARL) and Michigan Technological University (MTU). Contract identification information is given below.

| | |
|---|---|
| Contract Title: | Magnetic Resonance Imaging Studies of Process Rheology |
| Contract Number: | N00014-86-C-0724 |
| Work Unit Number: | Z400015SRS |
| Scientific Officer: | Dr. R.S. Miller |
| Period of Contract: | 9/30/86 to 9/30/89 |
| Princ. Investigators: | G.A. Lo (LPARL)<br>A.B. Kunz (MTU) |

## 1.1 BACKGROUND

Improved processing methods are needed to achieve reliable, continuous production of high quality propellant. This has created a need for new technical approaches to on-line monitoring of propellant materials for quality assurance and process control. Current techniques are either invasive (direct probes), limited to dilute systems (X-ray or ultrasonics), or only capable of providing information on near-surface conditions (optical). The relatively new technology of magnetic resonance imaging (MRI) has the potential to non-invasively determine structural and compositional parameters and flow velocities throughout the volume of a material. MRI has not yet been exploited for propellant processing, in part because of limitations from existing techniques designed for applications to aqueous systems. This program, which is a joint program between Lockheed Palo Alto Research Laboratory (LPARL) and Michigan Technological University (MTU), has been established to make the necessary advances in MRI Technology. This program combines advanced MRI development with fundamental rheological investigations of particle-filled, polymer-based materials and with detailed numerical modeling studies of interactions at the molecular level. This program is designed to provide the basis for new tools for on-line propellant process monitoring, new predictive models for the flow behavior of highly filled polymer systems, and critical design guidelines for continuous processing procedures.

## 1.2 OBJECTIVES

The overall objectives of the Program are to develop experimental and theoretical methods which will provide for improved methods of flow analysis as well as an improved understanding of the flow behavior of solid-particle-filled polymeric suspensions.

The objective of the experimental effort is to develop better methods to detect and characterize inhomogeneities in uncured solid propellant. The specific experimental methods to be studied in the Program are Nuclear Magnetic Resonance (NMR) and Electron Spin Resonance (ESR), both of which can be referred to by the general term Magnetic Resonance (MR) methods. The goal is to develop Magnetic Resonance Imaging (MRI) methods with 100 μm or better spatial resolution for stationary propellant samples and to develop methods for imaging the flow of uncured solid propellants in process streams.

The objectives of the rheological effort under this Program are (1) to determine the effects of rheological parameters on continuous processing and to use this information to help guide the magnetic resonance and theoretical efforts; and (2) to design flow systems and flow geometries for the Magnetic Resonance effort.

The objective of the theoretical modeling effort is to develop rigorous theoretical numerical models of macroscopic suspension flow in which the polymer-particle interaction physics are obtained from first principles. We believe this approach will provide a more thorough understanding of the origin and nature of the observed macroscopic behavior of concentrated solid-particle-filled polymeric suspensions. The plan is to link together models from the atomistic level (Quantum Mechanics) and the particle level (Stokesian Dynamics) to yield an integrated predictive method based as much as possible on first principles.

## 1.3 PROGRESS SUMMARY

A brief summary of the Program's progress is given below. Significantly more detail is provided in section 2 of this report, **PROGRAM STATUS**.

LPARL received a high-power, multi-nuclear (including hydrogen) nuclear magnetic resonance (NMR) spectrometer in September 1987 and completed installation of the unit in January 1988. By applying state-of-the-art multiple pulse NMR techniques, LPARL obtained the first-ever NMR images of solid aluminum particles (particle diameter = 5μm) in cured solid propellant simulant. LPARL designed and evaluated a simplified flow system for initial evaluation of NMR imaging methods and has ordered a pilot-plant scale (50 mm diameter) flow system for use in the coming year.

MTU completed construction of a high-field NMR spectrometer in February 1987 and, since then, has designed and tested two NMR probes for imaging solid materials using the magnetic resonance of nuclei other than hydrogen. MTU improved the design of the gradient coils on their sodium imaging probes, resulting in a three-fold improvement in resolution and began work on implementing multi-pulse methods for spectroscopy and imaging.

A continuous-wave electron spin resonance (ESR) spectrometer at MTU was configured for imaging, and initial studies were carried out to determine the potential of the technique for propellant analysis. The continuous-wave electron spin resonance (ESR) imaging spectrometer at MTU was used to evaluate several candidate ESR label materials in a number of imaging phantoms. The spectrometer was then modified to a low-power pulse-echo

configuration and initial studies of this setup were carried out. In the coming year, we will use both the continuous-wave and pulse-echo modes of the spectrometer to study the ESR characteristics of propellant simulants and candidate ESR label materials (when incorporated into simulants).

NMR Imaging of Samples at Rest. Initial NMR studies have been carried out with both cured and uncured propellant simulants. These simulants were designed to simulate the most relevant physical properties of the real propellant, and, where possible, used the same non-explosive components. They were prepared by Stevens Institute of Technology and the imaging results were correlated to their processing history.

*Polymer (Binder/Plasticizer) Components.* The LPARL NMR spectrometer was used to obtain NMR images of the polymer component of the above materials. These images showed clearly that concentration inhomogeneities, voids, and defects (cracks) are readily detectable. The current resolution in NMR images of the polymer (binder/plasticizer) components of modern, high-energy, highly plasticized propellant simulants was found to be on the order of 100 μm. The degree of homogeneity observed in NMR images of the plasticizer/binder in these samples correlated with their known processing history. We are in the process of developing unbiased statistical techniques for characterizing the homogeneity and structure of NMR images. These techniques or derivatives of them might eventually be used as feedback controls in processing applications.

*Solid Particles.* The gradient coils for the MTU sodium imaging probe were improved. Sodium NMR imaging was used to map the distribution of NaCl in a stationary sample of uncured, inhomogeneously mixed propellant simulant. The resolution in these images of the nuclei in the solid particles was about 1 mm (compared with 4 mm using the original MTU gradient coils). Coupled with a spectroscopic study of aluminum particles, these results indicate that, even with these improved gradient coils, aluminum NMR imaging, and imaging of solid particles in general, will require novel techniques; conventional methods will not give the desired resolution.

NMR Flow Imaging. A primitive couette cell was designed, fabricated, and tested to determine whether NMR imaging could detect flow induced changes in the structure of a viscous particle-filled fluid. Other studies (see above) had already shown that NMR imaging of solid particles would require new techniques. The objective of this study was to see how sensitive NMR imaging was to the variations in NMR relaxation times and nuclear density of the fluid which occur near solid particles. The results show that both these variations have an important role in determining contrast. The importance of relaxation time effects in these suspensions is especially encouraging since mix inhomogeneities can often be difficult to determine from density studies alone.

A preliminary flow system was set up within the LPARL NMR spectrometer and various flow imaging pulse sequences were evaluated. This study was focused on implementing published techniques for imaging flow, optimizing them for viscous fluids, and evaluating their utility. The results were encouraging -- we found that the mini-imaging system was capable of carrying out the flow imaging sequences, and we obtained valuable

information about the requirements of the next level of flow system which is needed for this Program. Future plans include setting up a pilot-scale laboratory flow system (50 mm diameter), further optimizing the flow imaging method, and widening the velocity detection range available to MRI.

Numerical Modeling Studies. Preliminary studies were carried out using the quantum mechanical (QM) and Stokesian Dynamics (SD) models in an uncoupled mode. The initial QM analyses of particle-filled polymeric suspensions yielded reasonable intramolecular polymer-polymer forces, and polymer-particle interaction forces. The attractive Van der Waals potential between polymer units was determined, along with the chain slip barrier. The SD model was also run in an uncoupled mode, and was used to predict how various flow conditions would affect the evolution of structure in a suspension.

The two models (QM and SD) were then linked together. In this mode, particle-particle interactions, as calculated by the QM model are allowed to influence the evolution of the overall suspension system, as calculated by the SD model. Parameters for the actual propellant filler materials -- ammonium perchlorate and aluminum metal -- were calculated by the *ab initio* QM method. However, for the sake of simplicity, studies with the coupled model used polyoxymethylene (POM) for the polymer matrix instead of Polyethylene glycol (PEG). POM has the same chemically functional groups as PEG but is a much smaller molecule, making it easier to generate SD input parameters from QM calculations.

To couple the models, a linearized Lennard-Jones (L-J) particle-particle attractive force was added to the SD model. Derivation of the ratio of L-J to hydrodynamic forces shows a dependence on the inverse of the particle radius. In polydisperse particle populations, therefore, the L-J force would be expected to exert a stronger influence on small (1-10 μm) particles than on large ones. Phenomena such as the tendency of particles to agglomerate or cluster could be affected by this force. This may be of particular interest in propellant systems because, in propellants, the fine particles often dominate the population. Since the L-J force becomes negligible when separation distances exceed about 50-100Å, only concentrated suspensions would be expected to show any significant effects of the L-J force.

## 1.4 SUMMARY OF PLANS AND PROJECTED PROGRESS

We plan to carry out the following studies during the remaining year of this program. Details of these plans are given in section 3 of this report, **PROGRAM PLANS**.

Rheological Studies. Prepare and characterize suspensions to be used in NMR flow imaging studies. Use the rheological information to aid in predicting and interpreting NMR flow imaging measurements in various shear rate ranges. Study the effect of suspension inhomogeneities on the rheological properties of the suspensions.

NMR. Construct pilot-scale flow system. Carry out flow imaging studies of 50 mm diameter flow system having flow velocities up to 10 cm/sec and fluid viscosities to 100,000 centipoise. Continue to develop statistical

methods for characterizing NMR image data. Design and evaluate advanced NMR imaging methods for fluids and particles. Acquire spectroscopy probe gradient accessory

ESR. Use continuous-wave and pulsed modes of ESR spectrometer to further evaluate ESR tracers for processing applications. Design and build flow imaging cell. Carry out flow imaging experiments.

Image Processing. Continue to evaluate available image processing methods and to develop novel combinations of these techniques for NMR imaging applications.

Theoretical Modeling. Use QM calculations to study particle-particle and particle-fluid interactions for Polyethylene glycol (PEG) with nitroglycerine (NG), alumina, and water. These QM results will be used to formulate simplified force-distance relationships which can be integrated into the SD model. Use SD model to study behavior of 3 to 10 particle systems under flow conditions of interest.

## 2. PROGRAM STATUS

### 2.1 Rheological Studies

The experimental rheological studies are being carried out at LPARL. The effort consists of four main tasks: (1) determination of the relevant rheological issues; (2) design and implementation of an experimental flow system; (3) selection of materials appropriate for study by NMR; and (4) rheological characterization of the selected materials.

Apparatus The LPARL rheology facility consists of a Rheometrics RMS-800 Mechanical Spectrometer. The rheology of concentrated suspensions can be characterized on the RMS-800 in steady shear, oscillatory shear, in a thixotropic loop, and in transient experiments. A photograph of the instrument is shown in Figure 1. Dr. Renée van de Griend, with a strong background in chemical engineering and experimental polymer rheology, joined the LPARL staff in January 1988.

Progress. Progress has been made in the following areas: (1) identifying the relevant rheological issues for continuous processing of solid propellants; (2) designing a flow system capable of delivering highly loaded suspensions under the flow conditions of interest; (3) selecting the material systems for use in the initial NMR flow imaging studies; (4) rheologically characterizing a number of fluids and suspensions as a function of material type and particle size; and (5) developing recommendations for flow systems and issues to be addressed by the experimental and modeling efforts.

*Relevant Rheological Issues.* The first task was to identify facilities studying continuous processing (i.e., apparatus, materials systems, applications), to determine the important rheological issues and processing parameters in real continuous processing systems, and to determine which of these issues could be reasonably addressed by the Program. The two facilities identified were the Naval Ordnance Station at Indian Head, Maryland (NOS/IH) and Stevens Institute of Technology (SIT), in Hoboken, NJ. A twin screw extruder has just been installed at NOS/IH. Initially, this system will be used for pilot-scale studies of non-energetic propellant simulants. Stevens Institute of Technology (SIT) has several types of mixing apparatus and extruders which are relevant to this Program. At both of these sites (NOS/IH and SIT), the main issues of interest are the homogeneity of the final product, detection and quantitation of processing-induced particle attrition, and "de-mixing" or shear-induced stratification. In terms of the relevance of material properties and processing parameters, the interests of NOS/IH are the most closely related to solid propellants; the non-energetic propellant simulants being studied by NOS/IH have the following characteristics: viscosities 4-40 kpoise, solids loading 70-90% by weight, throughput 25-750 lb/hour, velocities ~ 0.1 to 10.0 cm/s, and processing temperature ~ 150°F.

*Flow System Design.* The second task was the design and implementation of the experimental flow system. Design of the system is complete and all equipment has been ordered. Installation of the system will take place in the fall of 1988. The most important consideration in designing the flow system was selection of the pumping apparatus. The features that

are required for our flow system are as follows: (1) steady flow of high viscosity materials; (2) resistance to abrasive particles at high solids loadings; (3) flow rates within the NMR flow imaging limits (i.e., up to 10 cm/sec); (4) easy disassembly for fluid changes between experiments; and (5) the use of non-magnetic construction materials so as not to interfere with the NMR magnetic field. Screw extruders and screw volumetric pumps are generally considered the most appropriate type of equipment for transport of highly viscous suspensions in industrial applications. However, the high cost of this equipment makes it an impractical choice for our laboratory operation. It was determined that a MOYNO progressing cavity pump (80% stainless steel), manufactured by Robbins & Myers, was the only pump that could satisfy all of our requirements.

A schematic of the flow system is shown in Figure 2. The piping is constructed of stainless steel (pump to magnet), PVC (magnet insert), and high-pressure rubber hose (return from magnet to pump). All connectors are made of either stainless steel or PVC. There will be fittings throughout the system for sampling ports and temperature and pressure gauges. The pipe segment which runs through the magnet will initially be a straight 50 mm diameter cylindrical pipe. This configuration will later be modified to incorporate an abrupt contraction or expansion in the sampling region.

*Materials Selection.* The third task was the selection of materials for experimental study. The purpose of these initial MR flow experiments will be to characterize the hydrodynamics of concentrated suspension flows in the absence of the additional rheological complexities of a viscoelastic suspending fluid or strong particle-particle interactions. Therefore, the material systems for the initial flow imaging experiments will consist of homogeneous suspensions of non-interacting particles (i.e., no significant particle structuring in a quiescent fluid) in a Newtonian fluid. Fluids investigated for use in the MR studies included glycerine, corn syrup and silicone oil. Sized glass spheres and powders of aluminum and alumina were evaluated as potential candidates for solid fillers. Selection of appropriate fluids was mainly determined by viscosity considerations (i.e., laminar flow requirement, pumping capabilities, prevention of segregation, and NMR flowrate limits). Solids loading factors of interest included concentration, particle size, and particle size distribution. After studying a number of fluid / particle combinations, it was concluded that a suspension of sized glass spheres in corn syrup would be an adequate simulant for the initial MR imaging studies, and would have the added benefit of low cost and easy clean-up. After the initial MR flow imaging experiments with the corn syrup / glass spheres system have been completed, material systems will be changed to include a higher degree of rheological complexity. A polymeric binder will be used in place of the Newtonian fluid and particles which exhibit stronger interactions, such as agglomeration tendencies, will replace the glass spheres. These systems are discussed in more detail under **PROGRAM PLANS**.

*Rheological Characterization.* The fourth task is the characterization of the experimental fluids. This task has been completed for the corn syrup / glass spheres system. The purpose of this characterization was to determine which combinations of fluid viscosities and particle sizes

would be most appropriate for the flow experiments. Initial characterization studies were performed on a test matrix of different corn syrup / glass sphere suspensions. Available particle sizes of the glass spheres ranged from 10 to 200 μm. The viscosity of the pure corn syrup was approximately 2000 poise; lower viscosities were attained by the addition of water. Settling-rate studies were initially performed in order to determine viscosity limits for various particle sizes. Results indicate that the minimum fluid viscosities required for suspending the various particle sizes are 1000 poise for the largest particles, 100 poise for intermediate size particles (approximately 50 μm) and 10 poise for the smallest particles. Based on these results, concentrated suspensions containing only large particles ( >100 μm) will be eliminated from consideration for test fluids in the MRI flow experiments due to their prohibitively high viscosities. (We found that glass sphere suspensions in which the sphere diameters are > 100 μm generally have viscosities which are one to two orders of magnitude higher than the pure fluid.) However, the large particles will still be used to study the effects of particle size distribution and will be used in dilute suspensions for image analysis studies.

Rheological characterization studies were performed on suspensions of 10 and 50 μm particles in 120 poise corn syrup. Six suspensions were considered, with concentrations of 20, 40, and 60 weight percent of the two different particle sizes. Each mixture was characterized on the Rheometrics RMS-800 mechanical spectrometer in steady shear, oscillatory shear, and step shear reversal. The zero shear rate viscosities as a function of concentration are shown in Figure 3. The 20 and 40% suspensions appeared to be Newtonian in steady shear and the shear viscosities were equivalent to the complex viscosities. The 60% suspensions were shear-thinning and exhibited substantial accumulation of normal stresses with increasing shear rate, indicating a viscoelastic character. The complex viscosities for these suspensions were measured to be approximately half the shear viscosities.

The torque outputs, from which the shear viscosity is calculated, are shown in Figure 4 for step shear reversal tests. The linear response of the 20% suspension indicates that there is no shear-induced structure in the material. The non-linear responses of the 40 and 60% suspensions indicate an anisotropic structuring that occurs during shear. The non-linearity is much more pronounced in suspensions with greater solids loading.

The suspensions were characterized again, approximately four weeks after they were initially prepared, to determine whether or not they changed character with age. Visual inspection indicated a pronounced darkening of the suspensions, particularly in the 10 μm mixtures, while the appearances of the pure fluid and of the spheres in water remained the same. These observations suggest the presence of bacteria on the glass spheres which thrived in the corn syrup environment. Rheological measurements showed an increase in the viscosities of all fluids, probably indicating a small amount of water evaporation. The viscosity increase was much smaller in the 10 μm suspensions, lending further support to the assumption that some sort of biological degradation had

occurred. The results of the aging studies demonstrate the necessity of periodically characterizing the fluids during the MRI flow imaging experiments.

Recommendations for fluid systems for flow imaging experiments are based on the preceding characterization results. Concentrated suspension flow experiments will first be performed with a 20% solids system with particle sizes of 50 μm or less. Such a system does not exhibit structuring in the characterization experiments, and can thus be used as a baseline case. Studies will then continue with two 50 to 60% suspensions, one with 50 μm particles and one with 10 μm particles. These experiments will provide a determination of the effects of particle size and will be the first attempt at imaging a suspension flow with significant structuring. Particle size distribution studies can also be included by mixing known quantities of different size spheres. Finally, suspension flows with solids loadings of 80 to 90% with 10 μm particles in a low viscosity corn syrup will be studied. Due to the constraints imposed by the pumping capabilities and the fluid viscosities required to prevent sedimentation, these studies will not be extended to larger particle sizes.

## 2.2 Nuclear Magnetic Resonance Studies

2.2.1 LPARL. The LPARL NMR effort has made the following progress: The state-of-the-art NMR imaging spectrometer at LPARL was used to evaluate a number of flow imaging pulse sequences from the literature and to implement and test several of these sequences in a preliminary flow system. The results of this initial flow imaging study were used to design a pilot-scale flow system and to evaluate numerical and experimental methods for extracting flow and compositional information from NMR flow imaging data. We also used NMR imaging to study "goodness of mixing" in samples of uncured solid propellant simulant which had been processed for various lengths of time in a twin screw extruder. The NMR results correlated with the mixing time, indicating that NMR imaging can potentially be used to assess propellant quality in a process stream. The samples in this latter study were supplied by Stevens Institute of Technology.

LPARL NMR Facility. Installation of the LPARL NMR facility was completed in January 1988. This facility is equipped with a Bruker MSL-200 imaging NMR spectrometer, which is configured to carry out the full range of state-of-the-art multinuclear spectroscopy experiments, as well as mini-imaging and NMR microscopy.

The NMR microscopy system can handle samples up to 2.5 cm in diameter, has some multi-pulse capabilities for solids, rapid gradient switching times (~100 μsec), relatively high radiofrequency (RF) field strengths, an easy-to-adjust gradient system, and is capable of providing up to 10 μm resolution. This system is not presently able to handle flow-through geometries but this restriction can easily be removed if necessary, leaving its chief limitations to be limited sample size (25 mm maximum sample diameter) and limited solids imaging capabilities.

The mini-imaging system can handle samples up to 6 cm in diameter with a flow-through geometry and a maximum resolution of 100 μm. The chief

factors limiting the utility of the mini-imaging system for flow studies are the relatively long gradient switching times (3 msec), the difficult gradient adjustment procedure, and the low RF field strengths. These limitations have in part been overcome, allowing us to plan future flow NMR studies using the LPARL mini-imaging system as outlined below.

The LPARL spectrometer has a wide range of embedded data processing and image processing capabilities, which are further enhanced by the fact that the spectrometer is coupled to the central LPARL computing network.

NMR Imaging of Stationary Samples. The objective of this study was to develop and refine NMR methods for imaging the density of $^{1}H$ nuclei in stationary samples of propellant simulant, and to develop methods for determining the homogeneity of imaged samples and for reporting the results. Two sets of samples were used in these studies: (1) a set of Polybutadiene acrylonitrile-based (PBAN) propellant simulant samples supplied by Stevens Institute of Technology (SIT); and (2) a set of glycerine-based suspensions designed and prepared at LPARL.

*Sample Homogeneity.* Figure 5 shows four images of the samples from SIT. These samples consisted of approximately 60% by volume ammonium sulfate (AS) mixed into the highly viscous, liquid polymer PBAN. The mixing was done at SIT in their twin-screw extruder/mixer, and the four samples were taken from this apparatus at different locations along the screw direction. The images in Figure 5 were obtained by packing each sample into a 10 mm tube and electronically selecting a 250 μm-thick slice perpendicular to the axis of the tube. The pixel resolution in each image of Figure 5 is about 100 μm. The first sample, corresponding to the image in the upper left quadrant of Figure 5, was taken from the mixer at a point closest to where the raw materials entered the screw cavity and, hence, represents the least mixed of the four samples. The next three samples were taken at locations further down the cavity and represent increasing degrees of mixing. The degree of mixing is evident in Figure 5 in that the intensity variations become more homogeneously distributed and the dark features, which arise from clumps of unmixed ammonium sulfate or voids, become smaller as one reviews the images in increasing order. (The images are ordered with increasing sample mixing from left to right in the top row, and then again from left to right in the bottom row.) Thus, these NMR images correlate with the known processing history of the samples.

This data demonstrates how one might use NMR imaging in a qualitative manner to tell something about the quality of a processed propellant. We are interested in taking this a step further in an attempt to arrive at a more quantitative description of homogeneity. There are several reasons for doing this. First, the eye can only judge gross variations in homogeneity from one image to another. This is also a subjective process and might not catch the subtle variations which could be critical to product quality. Thus, a more quantitative analysis which approaches a less subjective description of homogeneity would be useful. Second, it would probably be impractical in a real processing environment for an operator to review a large number of images in real time. Any technique which reduces image data to a manageable number of relevant parameters would be amenable to automation. Finally, as we argue below, the proper treatment of the data may allow a substantial savings in the time it

takes to acquire it and analyze for homogeneity. This is of paramount importance since one of our goals is to develop truly real-time monitoring techniques.

One way to gain more statistically significant information about homogeneity from NMR images is demonstrated in Figure 6. In this figure, histogram plots of pixel intensities for each of the four images of Figure 5 are shown. These plots represent the relative number of pixels of each intensity as a function of intensity for the entire gray-level range of each image. Note how there are two distinct peaks in each histogram plot. The larger of the two is centered at lower intensities and arises from pixels which fall outside the limits of the circular object. This peak represents the pixel intensity distribution of random noise in the image and as such is referred to as the "noise" peak. The other peak represents the distribution of pixel intensities within the object and is called the "object" peak. In the least-mixed sample, this peak is broader than the noise peak and actually merges with it. As the degree of mixing increases across the series, the object peak narrows and separates from the noise peak. This behavior is due to a decrease in the range of pixel intensities within the object as the material becomes more homogeneous.

Histogram plots such as these provide a convenient means for characterizing NMR image data. One could extract a more quantitative description of the pixel intensity distribution by calculating the various moments of the distribution (e.g. average value, variance, etc.). Rather than pursuing this approach, we are developing an alternate method which shows merit and is based on spatial autocorrelation functions. A spatial autocorrelation function is a means of characterizing the distribution of sizes of features within an object. Mathematically, the autocorrelation function is calculated by summing over all relevant length scales the product of an image with itself after some displacement:

$$A(R) = \frac{1}{\sigma^2} \sum_r [I(r) - \bar{I}]\,[I(r+R) - \bar{I}] \qquad (1)$$

where:

$I(r)$ = image intensity at location r

$\bar{I}$ = mean value of the image intensities

$R$ = the displacement variable

$\sigma^2$ = the variance of $I(r)$

The autocorrelation function is a function of the displacement variable and can be plotted against this variable for inspection. If an object is perfectly homogeneous, and the autocorrelation function of its image is plotted against the displacement variable, the plot should decay immediately to random fluctuations about zero, controlled by the noise in the image. An object with internal features will have an autocorrelation function which decays slower and oscillates in some manner consistent with the feature sizes and the distribution of features. By examining the rate of decay and oscillations in autocorrelation functions, one should be able to distinguish a homogeneous object from an inhomogeneous

one. Furthermore, since the distribution of sizes of features is reflected in the autocorrelation function, valuable information about the nature of the inhomogeneity becomes available.

To demonstrate the technique, we have calculated simple autocorrelation functions from individual rows or columns extracted from NMR images. The first calculations were performed on a model system: pure glycerine and a suspension of carbon black particles in glycerine. These two images are shown in Figure 7. For various technical reasons arising from the physics of NMR imaging, this is a convenient system to work with since a wide range of image features can be produced with excellent resolution and signal-to-noise ratio. In the image of the suspension, dark regions arise from flocculated clumps of carbon black while bright regions represent higher concentrations of glycerine. Figure 8 shows pixel intensity histogram plots for these images. Differences in the width and position of the "object" peak in the two curves are clearly evident. Figure 9 shows individual traces of selected rows and columns through the two images. The autocorrelation functions for these selected rows and columns are shown in Figure 10. Note that the initial (leftmost) autocorrelation peak is broader for the suspension image than for the image of pure glycerine, indicating the presence of larger image features in the case of the suspension, which cause the autocorrelation function to decay more slowly. Note also that there are large oscillations in the curves for the suspension. These arise from the large, non-random features (dark spots) in the suspension image. These results clearly show the value of an autocorrelation treatment of image data.

Autocorrelation functions were also calculated for one row and one column from each of the four images in Figure 5. These results are plotted in Figures 11 and 12. The noticeable oscillations and slow decay observed in the autocorrelation function for the most poorly mixed sample (bottom-most curve) become progressively less evident as the samples become better mixed (moving up to the top-most curve). This reflects the break-up of large clumps of ammonium sulfate (corresponding to dark spots in the images) as the material becomes better mixed.

In the future, we plan to extend the autocorrelation calculations to two dimensions. We will use images of the carbon-black/glycerine system with varying degrees of homogeneity to test the method and quantitate the results. We are also working on an autocorrelation function treatment for one-dimensional (1-D) projections of an image along one axis. This has a distinct advantage over treatment of an entire two-dimensional (2-D) image in that it takes much less time to acquire the data for a projection along one axis compared to acquisition of a full cross-sectional image, thus speeding up the entire process by perhaps two or three orders of magnitude. The disadvantage in using projections is that certain information about how the inhomogeneities are distributed in an object is necessarily lost due to the averaging effect of acquiring only the projection. We plan to assess the relative merits and trade-offs between the full 2-D and the 1-D projection approaches.

NMR Flow Imaging. To carry out initial studies of NMR flow imaging, LPARL constructed a preliminary flow system, consisting of an upper reservoir, a vertical 38 mm diameter pipe, a lower reservoir, and a pump. Studies with this preliminary setup were focused on implementing

published techniques for imaging flow, optimizing them for viscous fluids, and evaluating their utility. The fluids used for this study were pure glycerine and water. The flow was studied in both directions; the pump was used to obtain upward flow and gravity was used to obtain downward flow. The NMR experiment which yielded the most useful information in this study was one whose objective was to nullify the effect of flow on the $^{1}H$ nuclei in the NMR probe, such that the $^{1}H$ density image obtained during flow would be identical to that obtained by ordinary techniques, had there been no flow. This is a necessary step in the implementation of velocity imaging by the method chosen in this study. As a result it was determined that (1) oscillations of the pump produced image artifacts which would be difficult to compensate for; and (2) gravity-driven flow would be inconvenient because of the need to maintain a constant gravity pressure differential. In addition, since the gravity-driven flow system is not a pressurized system, it is difficult if not impossible to avoid introducing significant numbers of air bubbles in the fluid, especially when the fluid is viscous. Because of the large difference in magnetic susceptibility between air and fluid, air inclusions significantly affect the NMR response. This sensitivity to voids may be advantageous in the long term, but since at the present time, we are primarily interested in developing and evaluating flow imaging methods, it is desirable to eliminate the inclusions. It was concluded that, in order to accommodate the range of flow velocities and the wide range of fluid viscosities of interest to the Program, a specialized, well-characterized pressurized pump system must be used. For this purpose, a pilot-scale recirculating flow system has been designed and ordered (see 2.1 Rheological Studies. *Flow System Design*).

LPARL experience to date indicates that the mini-imaging system should be capable of detecting velocities in the range of from about 1 cm/sec to about 25 cm/sec, depending on the materials, the flow geometry, and the velocity measurement technique. LPARL's future plans include efforts to widen this velocity detection range (see below, **PROGRAM PLANS**).

NMR Imaging of Particles. One of the most formidable impediments to imaging solid particles with NMR is the typically broad NMR resonance lines of such particles. To date, the solution to this problem has been to use stronger gradients with shorter gradient rise/fall times. This approach runs into tremendous difficulties when applied to large sample volumes such as in this Program. During 1988, preliminary studies of two new approaches were begun at LPARL. These two methods -- multiple pulse and multiple quantum NMR -- reduce the overall gradient requirements for imaging. Although it was possible to carry out preliminary analysis of these methods on the existing LPARL equipment, LPARL cannot proceed much further along these lines because it lacks a high-power solid-state imaging probe. The plan for 1988-1989 (see below, **PROGRAM PLANS**) is to transfer the basic methodology to MTU, so that they can develop the necessary imaging probe and experimental methods. The probe design and/or the probe itself will then be sent to LPARL for additional studies on the LPARL spectrometer.

2.2.2 MTU. Under this Program, MTU has (1) investigated several gradient coil designs; (2) built three NMR probes; and (3) carried out several NMR spectroscopy and imaging experiments. Some additional tasks

were funded jointly by this Program and by ONR contract N00014-86-K-0149: (1) development and proofing of the MTU NMR facility; and (2) development of dynamic gradient techniques.

Although the original plan had called for MTU to carry out flow imaging of solid particles by the second year, it took much more time and effort than expected to get the MTU spectrometer assembled and debugged. Because of this delay, it now makes more sense for MTU to concentrate on developing and testing methods for imaging particles in stationary samples than to develop particle flow imaging methods. However, the Program plan still calls for MTU to develop particle flow imaging methods. At a later date, the situation (i.e., progress made and capabilities of the two sites) will be reassessed to determine where particle flow imaging should be developed -- at LPARL or MTU.

NMR Probes and Gradient Coils. MTU has built three NMR imaging probes, all of which are designed for projection reconstruction imaging. The first imaging probe built by MTU under this Program was designed to image stationary samples using static magnetic field gradients. This probe was used to obtain $^{23}Na$ images of Polybutadiene acrylonitrile (PBAN) propellant simulant (discussed below, in Imaging). The second probe was designed for dynamic gradient experiments, but has not yet come into use because of problems encountered with the spectrometer electronics during switching of the dynamic gradients. The third probe was produced by replacing the gradient coils of the first probe with a solenoid-configuration gradient coil system. This probe also incorporates a motor-driven sample cell to study gravitational settling of particles in fluid suspensions. This probe is not yet complete, and therefore has not yet produced images for this Program.

NMR Spectroscopy. Comparison of $^{23}Na$ spectra from table salt and from LPARL-supplied PBAN propellant simulant confirmed that the NaCl is not dissolved in the simulant. $^{27}Al$ spectra of aluminum filings, annealed aluminum filings, and aluminum particles in PBAN simulant indicated that the aluminum particles in the simulant did not undergo much, if any, damage during processing.

NMR Imaging of Particles. Two sets of $^{23}Na$ images were collected of a PBAN simulant sample (15mm long x 9mm wide x 1mm thick) with and without a hole (9mm L x 2.5mm W). By improving the design of the gradient coils and the electronics of the console, the second set of images was much better resolved than the first set (~1mm compared to ~3mm, respectively). Images of the former sample obtained with the original and the improved gradient coils are shown in Figures 13 and 14, respectively.

MTU NMR Facility. The following tasks were funded jointly by this Program and by ONR contract N00014-86-K-0149. MTU completed integration of the basic elements of the spectrometer in May 1987. By June 1987, the MTU NMR spectrometer software and hardware had progressed to the point that simple experiments could be carried out. In order to demonstrate the multinuclear capability of the MTU NMR system, spectra of the following nuclei were collected: $^{23}Na$, $^{27}Al$, $^{6}Li$, $^{7}Li$, $^{63}Cu$, and $^{79}Br$. Since that time, a number of improvements have been made to the spectrometer software. MTU has installed Intermediate Frequency (IF) circuitry, which was to have enabled the spectrometer to carry out multi-

pulse line narrowing experiments while remaining in a broad-band mode. However, this circuitry is not yet functioning properly. Therefore, for the time-being, the multi-pulse methods are being implemented in a narrow-band mode.

## 2.3 Electron Spin Resonance Studies

The objective of the ESR effort has been to determine the feasibility of using ESR imaging for analysis of solid propellants (either cured or uncured). Progress has been made in the areas of (1) identifying candidate ESR label materials via ESR spectroscopy; (2) developing the ESR hardware, experimental methods, and software to image these label materials in propellant-like fluid suspensions; (3) imaging a number of solid specimens; and (4) upgrading the ESR spectrometer to a low-power pulsed configuration.

ESR Facility. A continuous-wave ESR spectrometer at MTU was adapted for projection reconstruction imaging, and the necessary data processing and image processing software was installed on the laboratory computer.

ESR Spectroscopy. Several candidate ESR label materials were identified and evaluated; these included:

- magnesium oxide (periclase) doped with divalent manganese
- zinc blende phase of zinc selenide, also doped with divalent manganese
- 1,1'-diphenyl-2-picrylhydrazyl (DPPH)
- triphenyl-verdazyl (TPV)
- reagent grade magnesium oxide (MgO) powder, with cubically symmetric trivalent chromium as an impurity
- crushed gamma-irradiated fused silica (quartz)

Based on the spectroscopy results, the first four label materials listed above were selected for use in imaging studies.

ESR Imaging. The initial ESR imaging effort produced images of the magnetic component of the electromagnetic (EM) field within the microwave cavity. These results were then used to help specify the sample dimensions to be used in subsequent imaging efforts. Subsequent efforts involved two-dimensional imaging of solid specimens and planar objects. Image resolution was on the order of 0.5 mm to 0.1 mm for samples containing TPV and DPPH.

## 2.4 Image Processing

The objective of the Image Processing (IP) effort under this Program is to investigate ways in which image processing and statistical data analysis techniques can enhance and simplify the extraction of information from NMR images. In this reporting period, our effort has been directed towards developing quantitative measures of image homogeneity. Once developed, such methods would permit a more unbiased comparison of the effectiveness of different mixing processes. We have investigated three methods. Our work on the first two methods -- Pixel intensity histogram analysis and Autocorrelation -- is discussed in detail in section 2.2.1, *Sample Homogeneity*. Although the pixel intensity histogram analysis approach is a good indicator of how well separated the

noise and signal are, and shows how much of the variation in signal intensity is due to random noise, it gives no information regarding the sizes of features in the image or their location. Autocorrelation analysis yields information on feature sizes but gives little or no information on the location of the features. The third IP method we have developed is a program call HOMOG which determines the sizes and locations of all features in the image. As HOMOG is currently configured, the following results are output: histogram of area sizes, area-weighted area mean, mean-square area, and standard deviation. The statistics are area-weighted in order to count each pixel in the area. Initial use of HOMOG to evaluate the four PBAN simulants (see Figure 5), has yielded encouraging results. As seen in Table 1, the area-weighted area mean, standard deviation, and mean square area all decrease as mixing time increases.

TABLE 1: Results of HOMOG analysis of PBAN simulant images (shown in Figure 5).

| Sample ID | Area-Weighted Area Mean | Standard Deviation | RMS Area |
|---|---|---|---|
| A | 15.3 | 7.4 | 17.0 |
| B | 14.4 | 6.4 | 15.7 |
| C | 13.5 | 4.7 | 14.3 |
| D | 13.3 | 4.5 | 14.0 |

Data which are stored for future processing include complete tables of feature size, intensity and location. This data could be post-processed in any number of ways to arrive at different measures of image homogeneity. The HOMOG technique shows great potential for analysis of image homogeneity and will be the subject of future studies within this Program. We will also continue to study autocorrelation and histogram analysis methods because of their applicability to image characterization in general.

## 2.5 Theoretical Modeling

There are two primary objectives of the modeling effort as proposed: (1) to exercise the QM model at MTU for atom clusters of relevant polymer binder and particle materials in order to provide interaction energies and relative forces of close polymer-polymer and polymer-particle units. This information will not only provide insights into the observed behavior of specific polymer suspensions of interest to ONR, but will (2) provide input material parameters for the coupled QM/SD model developed jointly by LPARL and MTU under this Program. This model is an attempt to bridge the modeling gap between atomistic-length and particle-length scales and to provide a fundamental approach to the prediction of bulk material response based on a fundamental knowledge of the components of suspensions.

2.5.1 Quantum Mechanics. Initial QM analyses of particle-filled polymeric suspensions have been carried out by the *ab initio* Hartree-Fock method at MTU. For the sake of simplicity, these studies used polyoxymethylene (POM) cluster models for the polymer matrix (in place of Polyethylene glycol), and ammonium perchlorate (AP) and aluminum (Al) metal as the particle materials.

These studies yielded reasonable POM-POM, POM-Al and POM-AP interaction potentials. Specifically: (1) POM-POM binding energies were estimated at 1.3 kcal/mole per unit cell, an equilibrium distance of 4.3Å and a chain slip barrier of 5.1 kcal/mole per unit cell, illustrated in Figure 15; (2) POM-Al binding energy was estimated at 23.7 kcal/mole per unit cell, and an internal binding energy of AP molecules in AP crystals was estimated at 19.5 kcal/mol per unit cell. The difference in binding energies between POM-AP and AP-AP shows that the dissolution of AP into POM is possible. This result is consistent with observations of AP solubility in Polyethylene Glycol (PEG) (PEG has nearly the same molecular structure as POM). The dissociation energy of AP into ions is 96.4 kcal/mol, indicating that, in POM or PEG, AP may be dissolved as AP molecules, and not as ions. The oxygen in the backbone forms a hydrogen bond with ammonium perchlorate. This attraction allows the polymer to coat the AP. The interaction is illustrated in Figure 16; (3) the POM-Al binding energy was estimated at 9 kcal/mol per unit cell, relatively strong as compared to the POM-POM, but weak as compared to the POM-AP. In this case there is sufficient attraction of the POM oxygen to the aluminum to allow the polymer to distort enough so that the separation of next nearest oxygens is commensurate with the aluminum lattice. The POM-Al interaction is illustrated in Figure 17.

The major finding of this study concerned how AP is incorporated into the propellant matrix. In PEG/AP propellants, it is generally believed that the AP forms a complex with the binder by first dissociating into ions, which then complex with the PEG. However, the QM calculations carried out by this Program show that, for the POM-AP system, the ionization energy for AP is much higher than the energy required for the whole AP molecule to form a complex with the POM molecule. This would indicate that the POM/AP complex would preferentially bind the AP molecule rather than its dissociation products. In order to confirm these results for the PEG/AP system, the QM simulations will be repeated in Year 3 for PEG/AP. The study will also include the effects of Nitroglycerine (NG) (the major constituent of the polymer binder in nitroplasticized polyether and crosslinked double base propellant systems), as well as the binding energies of PEG to aluminum oxide (commonly present on the surface of aluminum metal). The effect of dissolved water on the PEG/AP interaction will also be studied, since water from the environment is always present in propellant in small quantities.

The results of the QM simulations performed under this Program have been presented in the following publications:

"Ab Initio Study of the Interaction of Polyoxymethylene with Polyoxymethylene, Ammonium Perchlorate, and the Aluminum (100) Surface", M. Seel, A.B. Kunz, D.T. Wadiak, *Phys. Rev. B*, 37, 8915 (1988)

"Atomic Clusters and Cluster Models in Solid State Physics", *Int. J. Quantum Chem.*, M. Seel, invited lecture at the QCS symp. 1988 (in press).

2.5.2 Stokesian Dynamics Modeling. A two-dimensional (2-D) Stokesian Dynamics (SD) code, named SDWL© (for Stokesian Dynamics with Walls), was acquired through Dr. J.F. Brady of the California Institute of Technology. A three-dimensional (3D) Stokesian Dynamics computer code is also available from Brady, but it does not contain the shear field and close wall interaction features available in the 2-D code. The 3D code is available only with sedimentation (gravity) forces. The 2-D model has previously been tested for Newtonian suspending fluids and uniformly sized spheres under conditions of shear and sedimentation. The plan for this Program, therefore, is to use the 2-D model exclusively, because the 3D model cannot simulate the shear flow conditions of interest in processing situations. The maximum practical number of particles for a 2-D analysis ranges from 50 to 100 on the LMSC VAX/8650 and CRAY/XMP computer systems. A systematic study of code predictions of bulk suspension properties performed by Brady has shown that the use of 25 particle ensembles is sufficient to accurately simulate bulk (continuum) properties. We believe that Brady's prior work justifies LPARL's planned SD simulations with ensembles of up to 25 particles.

2.5.3 Coupled QM/SD Model. A prototype coupled Quantum Mechanical / Stokesian Dynamics (QM/SD) model was jointly developed by LPARL and MTU in 1988. The QM/SD model bridges the spatial scale range from Angstroms (Å) to micra (μm), or from the atomistic scale to the particle scale. Figure 18 illustrates the spatial scale of interest in the QM/SD model, outlined in the hashed box outline. It is known that the chemical makeup of particle suspension systems can have profound effects on the microstructure (the propensity to form particle agglomerates, for example), as well as the bulk response such as viscosity dependence on shear rate and temperature. In order to model the intermediate (on the order of μm) and large (on the order of cm) scale effects of the material interactions, it is necessary to modify the SD model to include non-hydrodynamic interactions that are material-dependent. Prior to this coupling effort, the SD model contained only hydrodynamic particle interactions that did not include parameters characterizing the chemical nature of the particles or the suspending fluid.

This integration allows us to study the effects of material-specific polymer and particle effects on the evolution of a particle suspension's microstructure. A natural consequence of an SD simulation is a prediction of the suspension's effective viscosity ($\eta_e$) as the microstructure evolves. So it is also possible to utilize the QM/SD tool to better understand the relationship between material specific microstructure and bulk material response.

QM simulations performed in 1988 on POM-POM, POM-AP and POM-Al interactions provided the basic QM parameters needed to make an attempt to spatially integrate the QM interaction effects into the SD simulation model operating at the micron length scale. The physical premise of the model is that solid particles in a polymer suspension can be coated with the polymer, and that the particle-particle interactions can be influenced by the polymer-polymer interactions between particles. The

polymer-polymer interaction takes the form of a Lennard-Jones (L-J) potential, where there is an attractive and repulsive region acting between particle centers at very close particle separation distances, as illustrated in Figure 19. Also acting at very close length scales are the hydrodynamic, or lubrication forces between particles. In the absence of the L-J force, the lubrication force is dominant, acting between particle centers, and is proportional to the particles' relative velocity component and the inverse of the separation distance acting along the centerline of the particle pair. The lubrication force is also illustrated in Figure 19.

Summary of QM/SD Results. A linearized L-J force-distance relationship for very close particle separation distances was developed and implemented in SDWL©. This force-distance relationship contains material-specific parameters which had previously been determined for POM-POM interactions. The ratio of L-J/hydrodynamic force amplitudes (ignoring the particle separation effects) can provide insights into the dependence of the forces on specific material and geometric parameters that characterize the system. The force amplitude ratio was found to be proportional to the fractional amount of polymer coverage on respective particles, and to the square of the density of polymer units (per unit particle surface area). The ratio is also proportional to the inverse of the particle radius, the fluid viscosity, and the shear rate. The exact form of this dependence is shown in Equation (5), developed below. The dependence on the inverse of the particle radius suggests that the L-J force dominates in small particles, and is negligible for large particles. This implies that in polydisperse particle populations, the L-J force would preferentially affect the small (1-10 μm) particles over the large ones. Phenomena such as the tendency of particles to agglomerate or cluster could be affected by this force. This is of particular interest in propellant systems where the fine particles dominate the population. Additionally, the L-J force becomes negligible when separation distances exceed about 50-100Å. Therefore, only concentrated suspensions would be expected to show any effects of the L-J force.

Since the SD model simulations for multiple particle (>2) systems are built up from single particle-pair interactions, it was necessary to test the physics of a single particle pair with and without the L-J force to confirm the physics of their interaction is correct. The most difficult situation to treat is when two particles approach one another. The difficulty arises when the singularity of repulsion is approached and the nonphysical particle overlap is to be avoided. A particle-pair test run to develop the necessary linearized L-J force-distance relationship and simulation conditions was chosen to force the close approach of two particles. Without the L-J force, the particle separation decreased smoothly, and the particles were repulsed by the lubrication force. However, when the L-J force was included, the particles attracted and were found to seek an equilibrium particle-particle distance, as shown in Figure 20. The simulation of the correct L-J physics comes at a price: the time step required to capture the close particle interaction requires a $10^3$ smaller computational time step than that required for the hydrodynamics simulations alone. This means that the CPU time required for any simulation including L-J forces would increase by $10^3$.

Although the use of Statistical Mechanics (SM) models in this Program was originally proposed as a method of integrating the QM results to the particle scale, the approach which we have followed (and which is described above) makes the QM results available directly to the SD model without the need for a SM model. However, the assumptions required for incorporating the L-J interactions into the SDWL© model ignore the effects of the fluid between the particles. If, in the future, the L-J forces are found to play a dominant role in particle-particle interactions and resultant material properties, it may be necessary to use SM methods to develop and quantify the effect of the fluid between the particles.

The results of this study to date are to be published in:
"Stokesian Dynamics with the 6-12 Lennard-Jones potential", M.J. Seel, D.T. Wadiak, A.B. Kunz, S.E. Hill, (in preparation) to be submitted to *J. Chem. Phys.*

Discussion. The relative simplicity of adding L-J forces to the SD model can be illustrated by examining Equation (2), the governing equation for the SD force balance between particles suspended in a Newtonian fluid:

$$\mathbf{R}\cdot\mathbf{U}^{*} + \mathbf{\Phi}:\mathbf{E} + \mathbf{F}p = 0 \qquad (2)$$

where $\mathbf{U}^{*}$ is a vector containing the translational and rotational particle velocity component relative to the bulk fluid translational-angular velocity evaluated at the particle center, $\mathbf{F}p$ is the non-hydrodynamic force (in our case the L-J force) acting along the particle-pair centerlines, $\mathbf{R}$ is the grand mobility matrix (dependent upon the instantaneous configuration of all particles), $\mathbf{\Phi}$ is the bulk linear shear flow and $\mathbf{E}$ is the constant symmetric strain rate tensor of the fluid. Equation (2) can be solved for the particle velocity vector $\mathbf{U}^{*}$

$$\mathbf{U}^{*} = -\mathbf{R}^{-1}\cdot\{\mathbf{\Phi}:\mathbf{E} + \mathbf{F}p\} \qquad (3)$$

Note that the non-hydrodynamic force $\mathbf{F}p$ is simply added to the hydrodynamic force $\mathbf{\Phi}:\mathbf{E}$ in Equation (3). Equation (3) can then be solved for particle positions by well known integration procedures and all that remains is to derive the form of $\mathbf{F}p$ for a L-J interaction.

The L-J force becomes active when the particles interact at close (<100 Å) particle separations. The forms of the force-distance relationship for the L-J force and lubrication force are illustrated in Figure 19. The procedure for integrating the L-J 6-12 (attractive force $\propto 1/r^{6}$, repulsive force $\propto 1/r^{12}$) for polymer-polymer unit interactions over the particle surfaces is relatively straightforward, and results in an inter-particle force-distance relationship of the form:

$$F(\xi) = -F_0\left[\left[\frac{\xi_0}{\xi}\right]^{4} - \left[\frac{\xi_0}{\xi}\right]^{10}\right] \qquad (4)$$

where $F_0$ is the amplitude of the L-J force, given by Equation (5):

$$\frac{F_0}{6\pi\mu a^2\dot{\gamma}} = \frac{\pi^2 q^2 \varepsilon a^2 r_e^2}{6\pi\mu a\dot{\gamma}} = \frac{1}{\dot{\gamma}^*} = \frac{\pi q^2 \varepsilon \xi_0^2}{6\mu a\dot{}} \qquad (5)$$

Note that "a" in Equation (5) is the particle radius, $\xi$ is the non-dimensionalized (by the radius a) particle surface separation distance, q is the number of polymer units per unit particle surface area, $\xi_0$ is the nondimensional QM polymer-polymer equilibrium distance, $r_e$ is the L-J equilibrium separation distance, $\varepsilon$ is a parameter describing the attractive force well depth, $\mu$ is the fluid viscosity, $r_e$ is the L-J equilibrium distance and $\dot{\gamma}$ is the bulk applied shear rate.

The ratio of L-J/hydrodynamic forces reveals the relative effect of the L-J force. Note that because the force ratio is proportional to 1/a, the L-J forces dominate as the particle radius decreases. This makes sense physically, because non-hydrodynamic attraction/repulsion phenomena would dominate in suspensions with very small particles (e.g., colloid suspensions). Note also that the L-J force increases (1) as the density of polymer coverage increases; and (2) with the square of the equilibrium separation distance. The force ratio is on the order of $10^4$ to $10^6$ for the POM coatings, typical shear conditions and particle separations of less than about 50Å or 60Å.

A simple particle-pair model was developed for an SD simulation to demonstrate that the model incorporates the correct particle-pair interaction physics. Since n-particle interactions are built up from particle-pair interactions, this is a critical test of the validity of particle ensemble interactions. The parameters listed in Table 2 were arbitrarily chosen for the test. The L-J force-distance relationship was linearized for inclusion into the SD code, and simplified for acceptable solution convergence behavior.

TABLE 2: Parameters for the 2 particle simulation

| Parameter | Symbol | | Value |
|---|---|---|---|
| Particle radius | (a) | = | On the order of 1μm |
| Fluid viscosity | (μ) | = | 0.1 kg/m-s |
| L-J equil. | ($r_e$) | = | 4Å (polyoxymethylene units) |
| L-J attraction | (ε) | = | $10^{-22}$ joules |
| Polymer density | (q) | = | $5.6\times10^6/m^2$ |
| F(L-J)/F(hydro) | ($1/\dot{\gamma}^*$) | = | $10^6$ |

Figure 20 illustrates the initial particle-pair positions. The lower particle is constrained by a wall (lower boundary). Both particles are given a gravity body force of O(1). Figure 20 shows the particle separation distance $\xi$ as a function of time as the particles approach. Without the L-J (or van der Waals) force, the separation distance decreases smoothly as the repulsive hydrodynamic force dominates. However, when the L-J force begins to be effective (i.e., at particle separations of 50Å), the attractive force draws the particles together

strongly, and reaches a new, closer equilibrium distance. The ringing in the $\xi$ vs time curve in Figure 20 is due to the lack of an effective numerical "dashpot" in the linearized L-J force-distance model. The eventual decay of the separation distance to an equilibrium position over time is due to the damping effect of the lubrication force, which is proportional to the relative velocities of the particles. Figure 21 plots the resultant L-J and gravity y-component of forces on the particle pair (the lubrication forces are not included in this illustration).

The results of the particle-pair test show that the appropriate physics are modeled, and the appropriate behavior was obtained for two particles interacting with lubrication, gravity and L-J forces. Because of the difference in length scales of the L-J vs. the lubrication forces, it was necessary to reduce the normal time step by a factor of $10^3$ in order to capture the L-J interactions (The time step naturally scales with the distance scale for these processes). The impact is that significantly more computer CPU time is required to simulate hydrodynamic interactions when L-J interaction physics are included.

## 3. PROGRAM PLANS

### 3.1 Rheological Studies

Materials Selection. LPARL will coordinate the requests for simulant samples, and will either prepare the samples, obtain them from Stevens Institute of Technology (SIT), or supply the raw materials to the various efforts at LPARL and MTU. LPARL will also coordinate requests for rheological characterization and will decide whether to carry out these measurements at LPARL or to have SIT do the analyses.

Plans for coupling the rheological characterization experiments with NMR flow imaging experiments for the first stage experiments at LPARL are as follows: (1) prepare sized glass spheres / corn syrup suspensions of varying concentrations, particle sizes, and particle size distributions. (2) characterize samples on the RMS-800 to determine the influence of various solids loadings factors on viscosity and degree of pseudo-plasticity. (3) utilize rheological information in predicting and understanding NMR flow experiments in various shear rate ranges.

We will move towards using simulants composed of PEG/Aluminum as soon as possible.

As noted above, under **PROGRAM STATUS**, the second stage of the experimental rheology effort will involve the study of rheologically-complex materials in entry and exit flows. In this stage, polymeric binders such as Polyethylene Glycol (PEG) will be used as the carrier fluid of the suspensions. The suspension systems we will be studying are related to systems being studied at SIT, representing a collaborative effort. Phenomena to be studied include (1) particle effects and interactions, such as flocculation and agglomeration; and (2) the effect of mixing inhomogeneities on the rheological properties of the suspensions. Later MR studies will use these more complex suspensions.

### 3.2 Nuclear Magnetic Resonance Studies

The plan for the NMR effort for late 1988 to early 1989 is as follows:
LPARL: (1) construct a pilot-scale (50 mm diameter) flow system capable of handling flow velocities up to 10 cm/sec and fluid viscosities up to 100,000 centipoise. (2) conduct NMR imaging studies of a flowing suspension in a straight pipe with and without constrictions.
(3) continue to develop statistical methods for determining and characterizing / reporting homogeneity as viewed by the NMR data. (4) in collaboration with MTU, design and evaluate advanced NMR imaging methods for particles and fluids. In this development and evaluation effort, we will consider advances in theoretical analysis, experimental pulse sequences, and image processing / image interpretation methods.
MTU: (1) obtain $^{27}Al$ NMR images of stationary solid propellant simulant samples by multi-pulse line-narrowed imaging and/or multiple quantum imaging to evaluate, compare, and improve particle imaging capabilities. (2) design/construct an NMR imaging probe for these multi-pulse imaging studies.

### 3.2.1 NMR Spectroscopy / Imaging of Fluids.

Sample Homogeneity Study. One specific goal of the LPARL NMR effort is to produce a more quantitative description of what can be learned with proton imaging of suspensions. LPARL will determine the experimental matrix sample requirements and will carry out NMR Imaging experiments (measure the density, $T_1$, and $T_2$ of $^1H$ nuclei) of SIT-supplied and LPARL-supplied samples. The objective is to develop the means to statistically analyze intensity variations in these images and to relate the results to suspension homogeneity. LPARL will work closely with SIT for sample characterization and data analysis. Whenever possible, the samples will be made available to MTU; their NMR particle imaging and/or ESR work may lead to complementary information. LPARL will develop a meaningful mechanism for determining and characterizing/reporting homogeneity, and will correlate the results to the sample history and processing parameters provided by SIT. Preliminary progress in this area is reported above (see section 2.2, **PROGRAM STATUS**, Nuclear Magnetic Resonance Studies).

NMR Flow Imaging. So far, LPARL has successfully implemented one NMR flow imaging pulse sequence using a 38 mm diameter pipe. In the coming year, LPARL will continue to develop flow imaging methods for binder components. More work is needed to refine techniques and to extend them to more viscous and highly-filled systems. The objectives for the LPARL flow imaging effort are: (1) construct and install a pilot-scale flow system. (2) refine the NMR imaging technique used for refocusing flow velocities. (3) evaluate alternate flow imaging pulse sequences. (4) carry out NMR flow imaging (i.e., density and velocity images) of a straight pipe with and without constrictions. (5) evaluate the utility of NMR relaxation times as an image contrast mechanism.

### 3.2.2 NMR Spectroscopy / Imaging of Particles.

NMR Spectroscopy. LPARL will further evaluate multi-pulse and multiple-quantum methods for imaging solid particles. This evaluation will involve theoretical and experimental development of these imaging modalities. LPARL will conduct only preliminary spectroscopy experiments (along the lines of LPARL's previous work) until either an $^{27}Al$ solids imaging probe or a spectroscopy gradient accessory becomes available (see below, Spectroscopy Probe Gradient Accessory).

MTU will implement multi-pulse capability on their spectrometer and will carry out line-narrowed $^{27}Al$ spectroscopy of solid aluminum particles on cured and uncured propellant simulants.

Multi-Pulse NMR Imaging of Particles. The plan for particle imaging is to have MTU incorporate multi-pulse $^{27}Al$ line narrowing into the NMR imaging experiment and to use this method to image particles in stationary samples of propellant simulant. This approach will build on the $^{27}Al$ line narrowing spectroscopy and preliminary imaging experiments carried out by LPARL in early 1988. (Multi-pulse line-narrowing spectroscopy is a way of applying a series of precisely timed and phased RF pulses such that atomic level magnetic interactions which give rise to the broad resonance lines are negated.)

In terms of hardware, MTU must build a high-power multi-pulse imaging probe and finish installing IF circuitry in the MTU spectrometer. Once multi-pulse techniques are working on the MTU system, imaging techniques to exploit them will have to be developed. Although some multi-pulse imaging sequences have been reported, this technology is by no means completely worked out. Multi-pulse spectroscopy becomes more difficult when the sample is not in a homogeneous magnetic field, which is precisely the case in NMR imaging, where spatial encoding is achieved through the use of inhomogeneous magnetic fields. In fact, the preliminary LPARL multi-pulse imaging study reported above showed that even low-power magnetic field gradients make multi-pulse imaging a non-trivial task, making it doubtful whether it will be possible to get acceptable images by merely "switching on some gradients" with multi-pulse line narrowing. It will be an especially challenging task to get rapid results out of the multi-pulse imaging effort, and LPARL will assist MTU in this effort in whatever way(s) possible.

3.2.3 NMR Spectroscopy Probe Gradient Accessory. The initial $^{27}Al$ line-narrowing multi-pulse imaging experiments carried out by LPARL (see above, **PROGRAM STATUS**) demonstrated the utility of employing LPARL's specialized spectroscopy probes to evaluate novel imaging sequences instead of building specialized probes for each experiment. In the $^{27}Al$ imaging trials, LPARL was limited to the low-power magnetic field gradients available from the mini-imaging gradient system. As a result of the success of these experiments, LPARL has decided to acquire a spectroscopy probe gradient accessory. The envisioned gradient system will be able to be used with any of the spectroscopy probes, and will be capable of generating medium-strength magnetic field gradients (10-15 G/cm). Commercial vendors capable of custom design and construction of this hardware have been contacted and have submitted cost estimates. We expect to order the accessory in the near future.

3.2.4 Processing of Velocity/Positional-Encoded Images. NMR flow imaging data contains three dimensions of velocity information, three dimensions of positional information and several dimensions of chemical information. To date, common approaches to the problem of deconvoluting the information have been to choose simplified flow systems where there is only one significant velocity component and where the chemical composition is homogeneous and is well known. This approach, though acceptable for initial studies, will not be adequate for the long term for the suspensions and applications of importance to this Program. Although there are ways of designing the NMR flow imaging experiment such that only one component of velocity is collected at a time, this approach is only appropriate for steady-state flows. We believe it will eventually be necessary to develop a generalized numerical approach for deconvoluting the velocity and positional information from the NMR imaging data. During the coming year, we will be studying this problem from several different perspectives to arrive at the best solution.

3.3 Electron Spin Resonance Studies

The plan for the ESR effort for 1988 to early 1989 is as follows: (1) construct a pulse-echo ESR imaging spectrometer. (2) design an experimental matrix for both static and flow imaging, determine sample needs, and transmit to LPARL. (3) further evaluate tracers (e.g., MgO,

TPV, DPPH) for ESR imaging applications. (4) carry out static ESR imaging experiments. (5) design & build a flow imaging cell. (6) carry out flow imaging experiments.

## 3.4 Image Processing

The plan for the Image Processing (IP) effort for late 1988 to early 1989 is as follows: (1) Enhance the ability of the IP methods described above (section 2.4) to quantify image homogeneity, (2) Develop new combinations of standard IP methods to optimize extraction of chemical and processing information from NMR imagery, (3) Incorporate the image analysis methods into our VAX-based NMR data analysis program, FTNMR.

We will evaluate various ways of post-processing the HOMOG results to determine the best ways of quantifying image homogeneity. For example, we will calculate the various moments of the spatial distribution of selected feature sizes (or ranges of size) and evaluate the effectiveness of using these moments as homogeneity criteria. We will also evaluate the effects of modifying the feature identification criteria used in HOMOG.

We plan to evaluate new combinations of standard IP methods for their ability to extract specific chemical and processing information from NMR imagery. Our approach will be to combine standard, well-proven IP methods in novel combinations, according to the somewhat unique information content of the NMR data and according to our specific needs (HOMOG is a successful result of such an effort).

Finally, we plan to incorporate the image processing methods described previously (see section 2.4) into the FTNMR program to allow more advanced evaluation of these techniques on a greater number of data sets. FTNMR is a commercially available NMR data analysis program. By using this program for data analysis, we free up the NMR spectrometer for experimental work. In addition, by having the FTNMR program on the central LPARL VAX system, we are able to apply the powerful capabilities of LPARL's extensive lab-wide software library to NMR data analysis. FTNMR also facilitates communication of NMR data to other groups, such as the Digital Image Processing Laboratory, for further analysis and for method development.

## 3.5 Theoretical Modeling

The primary objectives of the LPARL and MTU modeling task are stated in section 2.5 of this report. Future objectives of this effort should remain the same, although the specific tasks required to carry out the objective will change as outlined below.

3.5.1 QM and SD Models. Strategic system propellant lacquers are Newtonian. However, because of the high solids loadings in solid propellant mixes, the inter-particle forces lead to non-Newtonian bulk response. The current SD model can treat these systems with good results as long as all the particles are the same size. However, because the types of suspensions of interest to this Program typically have several particle size populations, the ability of the current SD models to

realistically assess the effect of multiple particle sizes is currently limited. The problem of introducing multiple sphere sizes into the SD model has been looked into and is discussed later in this report.

The investigation of particle-polymer cluster interactions of specific material systems by Quantum Mechanical (QM) calculations will be continued by MTU. The material systems to be examined are PolyOxyMethylene (POM)-Aluminum, POM-NaCl, POM-$NH_4SO_4$, Polyethylene Glycol (PEG)-Nitroglycerine (NG)-Alumina, and water. The detail in these studies will be increased to allow determination of polymer-particle slip barriers so that statistical mechanical methods may be used to dynamically model the large-scale system behavior. This will result in the development of simplified force-distance relationships for wetted and unwetted particles at small distances (Angstroms) to be integrated into the SD model of particle-particle interactions.

As mentioned in **PROGRAM STATUS**, LPARL and MTU have created a coupled QM/SD model to investigate the effect of the very close particle-particle interactions in highly concentrated suspensions. The relative importance of the L-J interaction on the formation and behavior of particle agglomerates and clusters, as well as bulk response under a limited selection of external loads and materials simulating typical processing conditions is of particular interest, and will be investigated by LPARL in Year 3.

Test runs of the QM/SD model with small ensembles of particles (5 to 10) before more extensive runs are planned for 1989. These test runs are intended to provide the basis from which we can estimate CPU and memory usage requirements for more extensive simulations. From a scientific standpoint, the test runs should also provide limited insights into the relative importance of the van der Waals forces in the evolution of a suspension microstructure. For example, simulations of 5 to 10 particles with and without van der Waals forces could indicate whether the system response changes and if the bulk properties (such as the effective viscosity) change with van der Waals forces.

The small time step limitation (hence, extensive CPU requirements) for the QM/SD model limits the scope of modeling studies within this Program, and therefore only small ensembles will be exercised. However, the next step in the exercise of the QM/SD model, which is not planned for this Program, would be to systematically examine variations in the van der Waals parameters, hydrodynamic parameters, and suspension composition (e.g., particle fraction) to explore the behavior of the suspension under the influence of van der Waals forces.

3.5.2 Finite Element Flow Dynamics Modeling. LPARL does not currently have a Finite Element (FE) code capable of modeling non-Newtonian fluid flow, but it does have Finite Difference (FD) software (Microcompact©, by Innovative Research Inc.) available to model these flows. LPARL will use this FD software, if needed, to predict material response under the conditions expected in the NMRI flow experiments planned for Year 3. The objective will be to predict the state of the fluid for selected NMR flow probe geometries and flow conditions. These results will be used (1) for evaluation of potential NMR flow probe designs; (2) to aid in the interpretation of NMR results; and (3) for comparison with the NMR

results. MTU has FIDAP©, a Finite Element code for non-Newtonian flow simulations available for use if required.

## 4. COLLABORATIONS WITH OTHER PROGRAMS

### 4.1 Massachusetts Institute of Technology

In addition to our collaboration with SIT, ONR has expressed an interest in having this Program work with Massachusetts Institute of Technology (MIT) in two areas: (1) to use the MIT flow dynamics FE code to analyze our NMR flow system and to augment our macroscopic theoretical modeling effort; and (2) to study the process rheology of Polyisobutylene (PIB) based fluids. We are in full agreement with the former suggestion. We plan to study the MIT code to determine its relevance to the various aspects of our Program and to decide whether to install the code on one of our computer systems or to have MIT do the desired analyses for us.

With regard to the MIT study of PIB, our understanding is as follows: ONR would like to set up an integrated program to study the rheological and processing properties of a single fluid using a number of different techniques and a number of laboratories. The overall objectives of the envisioned program are to compare the performance of different experimental analysis methods and numerical modeling codes, and to determine the role of elasticity on mixing and processing. As we understand it, PIB was chosen for this study because it is already very well characterized (it has a constant viscosity over a wide range of shear rates and exhibits high elasticity) and because MIT has a large amount of PIB which it is willing to prepare and distribute to the research groups involved, so that everybody will be working with exactly the same material. Dr. R. Armstrong (MIT) has volunteered to mix a large quantity of PIB-based fluid and to have the fluid characterized by associates in the United Kingdom and Australia. Dr. H.H. Winter (University of Massachusetts, Amherst) will carry out rheological characterization of the fluid, and SIT will measure the behavior of the fluid in their process simulator as a function of mixing speed. In addition to these experiments, SIT and MIT will model the behavior of the fluid in the SIT process simulator using their elastic and viscoelastic 2-D flow dynamics FE computer models, respectively. SIT has designed a process simulator for this study which is several inches high, has an outer non-rotating cylinder which is 5 to 6 inches in diameter, and a rotating, elliptical kneading element in the center of the sample cavity.

After reviewing the plans for the integrated PIB study, LPARL has come to the conclusion that this Program could not make very significant contributions to the PIB study in its current form. Our decision was based on a number of factors, the most important being the fundamental differences between the fluid behaviors which are of importance to the two programs. PIB represents an important class of experimental fluids. It is ideal for use in programs in which theoretical models of polymeric behavior are being developed or tested, because it provides an experimental measure of elasticity in the absence of shear-thinning or inertia. The objective of the LPARL program is to study the behavior of concentrated suspensions; for these systems, the high solids loading and fluid-particle interactions dominate the flow behavior. If PIB were used as the suspending medium, its useful properties (i.e. constant viscosity and high elasticity) would be overshadowed by the presence of the solids. Therefore, the use of PIB as a base fluid for the suspensions would not provide any connection with the MIT program because the rheological

behavior of the filled system would bear no similarity to the unfilled system. Second, it would be difficult to redesign the process simulator so that the kneading process could be analyzed with the available magnetic resonance imaging equipment. The simulator would have to be scaled down by at least 50% and the drive mechanism would have to be completely redesigned to position the motor five feet or more from the simulator sample cavity, outside the primary fringe field of the magnet. In addition, all simulator components but the drive motor would have to be nonmetallic. Third, all of the NMR flow imaging methods we are currently using are designed for analyzing flow through a much simpler geometry (e.g., a straight pipe with or without constrictions). The flow geometry used in the PIB study is much more complicated and would require a significant advance in flow imaging capabilities. Although we are working on the design of new flow imaging methods, it will be some time before we can reliably determine 3-D velocity components in an arbitrary geometry. Finally, since PIB is a transparent fluid, it is amenable to optical flow analysis methods, whose sensitivity and accuracy far exceed that of NMR flow imaging. Therefore, MR flow imaging would not provide any new information.

We plan to stay abreast of the PIB study and will periodically reconsider whether involvement of this Program is warranted.

## 5. SCHEDULE

The Revised Program Schedule for 1988 to early 1989 is provided as Attachment A. The revised program plan will be updated periodically.

(a)

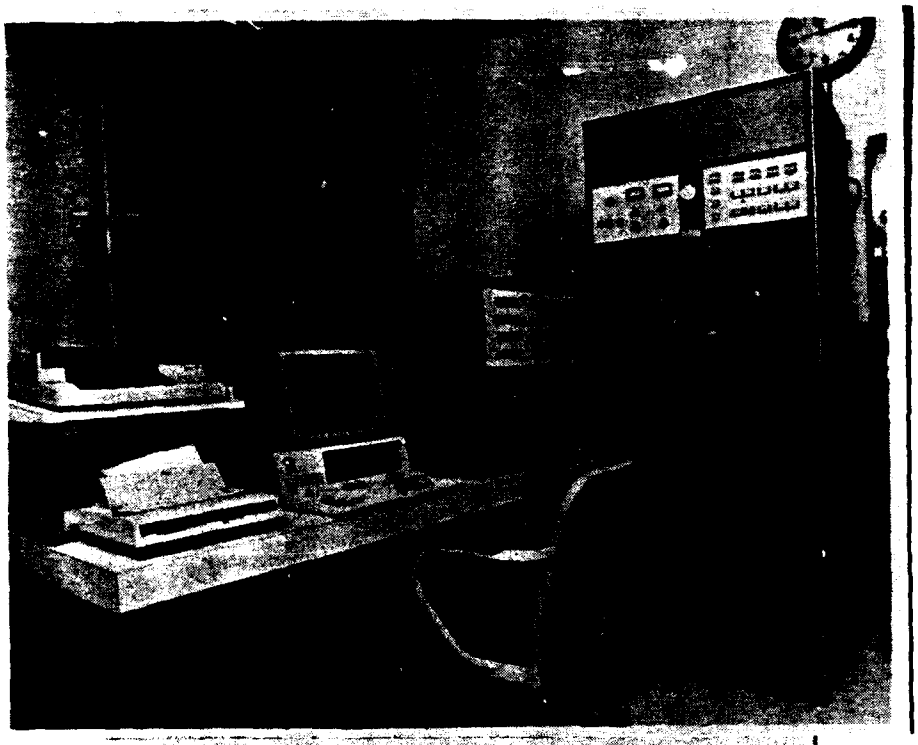

(b)

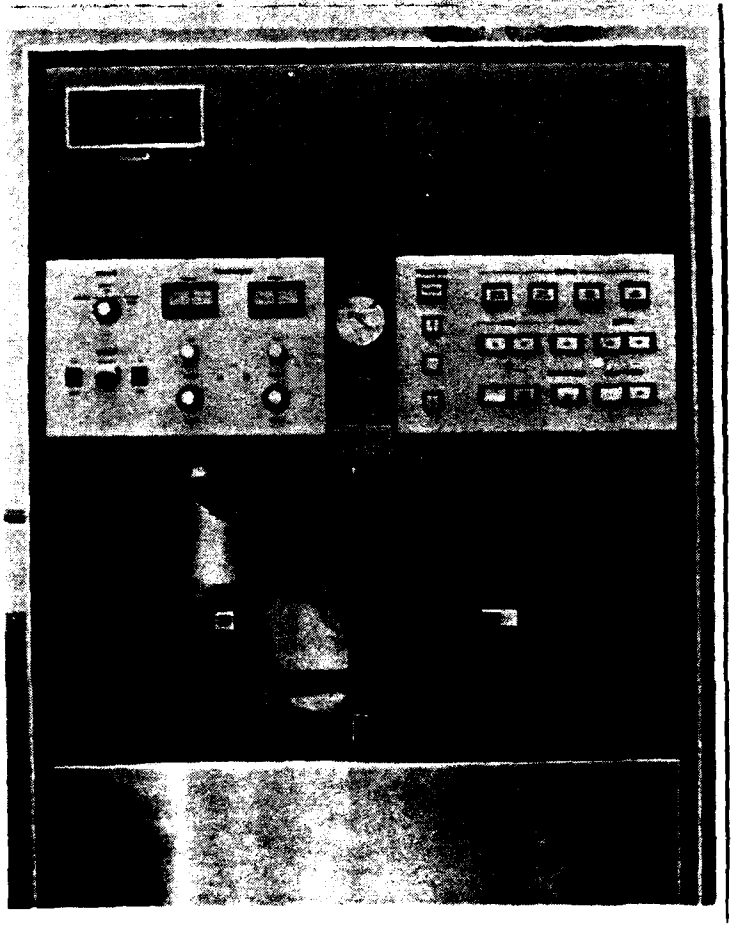

Figure 1: Rheometrics RMS-800 Mechanical Spectrometer (a) complete instrument, (b) test station with parallel-plate fixture installed.

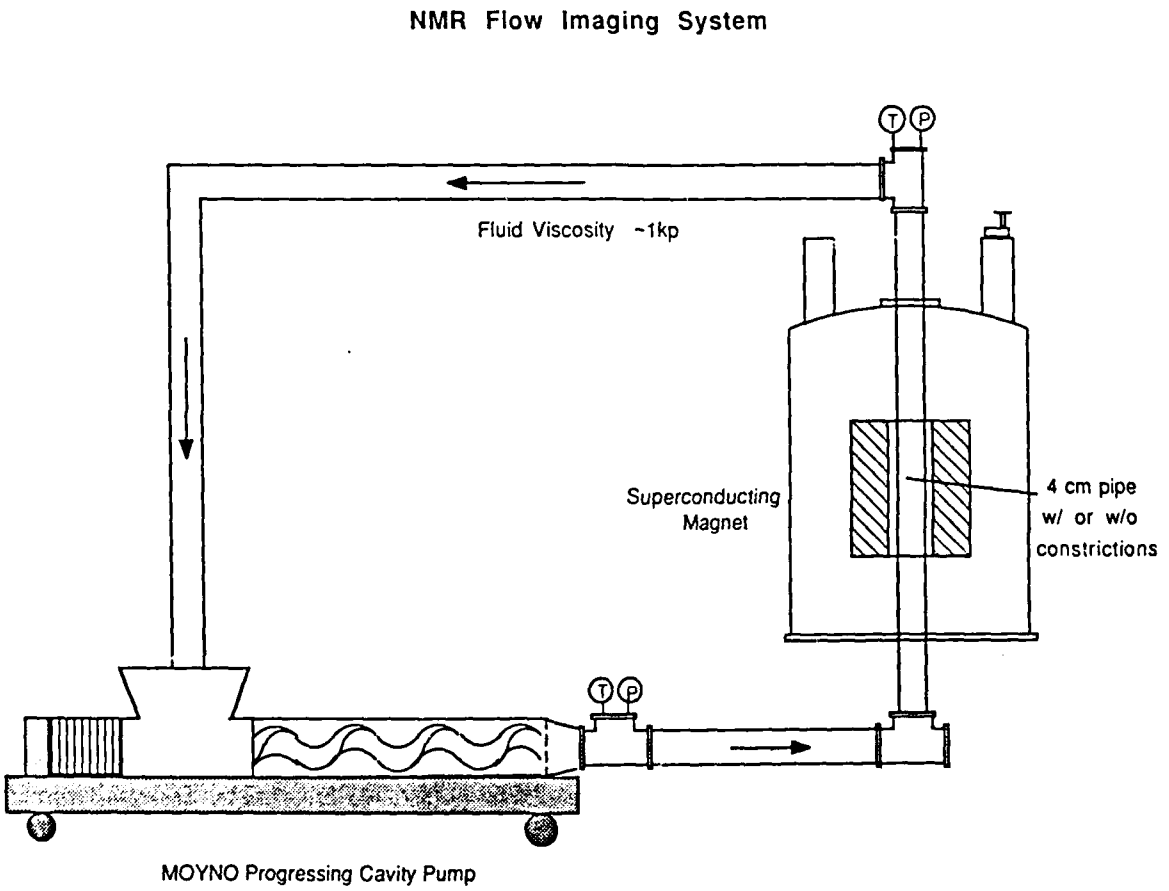


Figure 2: Schematic diagram of MRI flow system

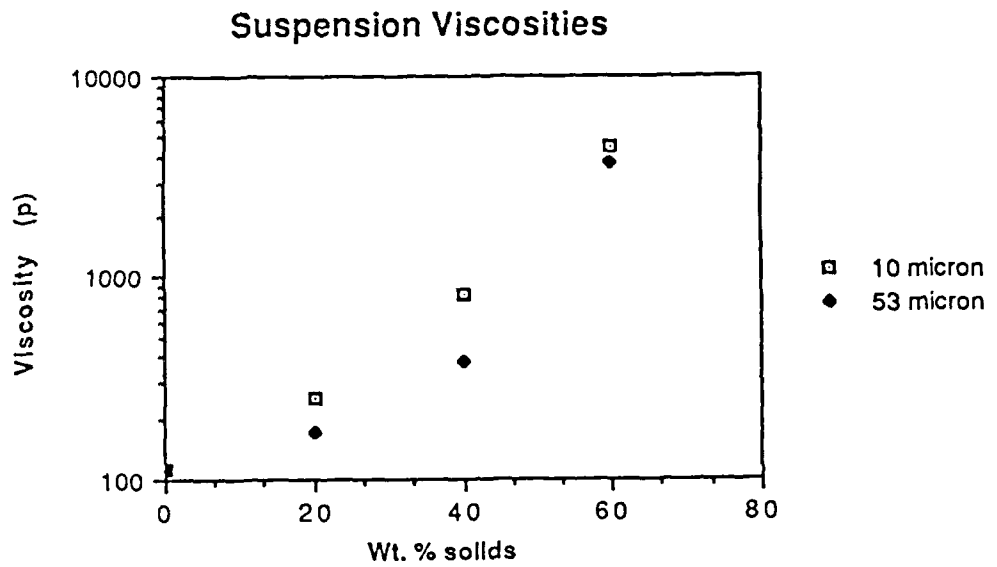


Figure 3: Zero shear rate viscosity results for suspensions of glass spheres in 120 poise corn syrup

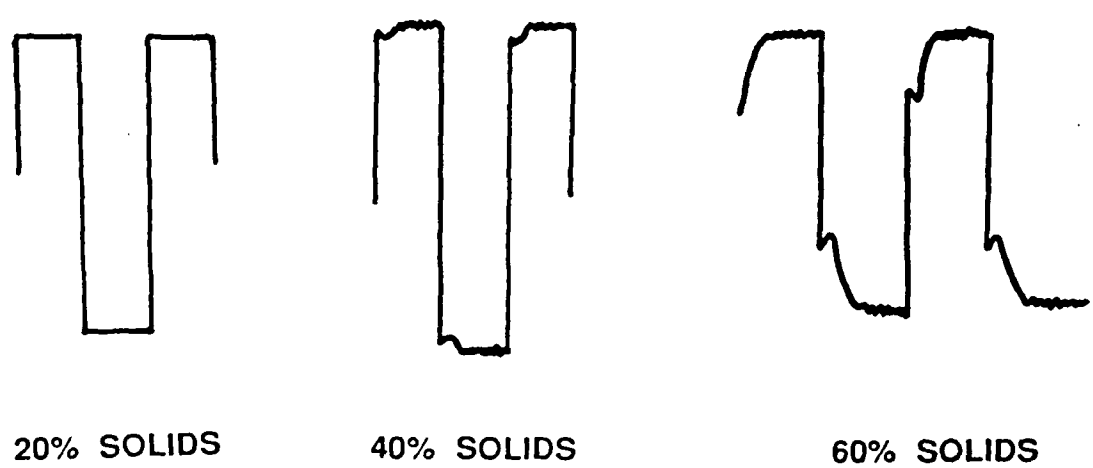


Figure 4: Torque output of step shear reversal tests for suspensions of 10 μm glass spheres and corn syrup

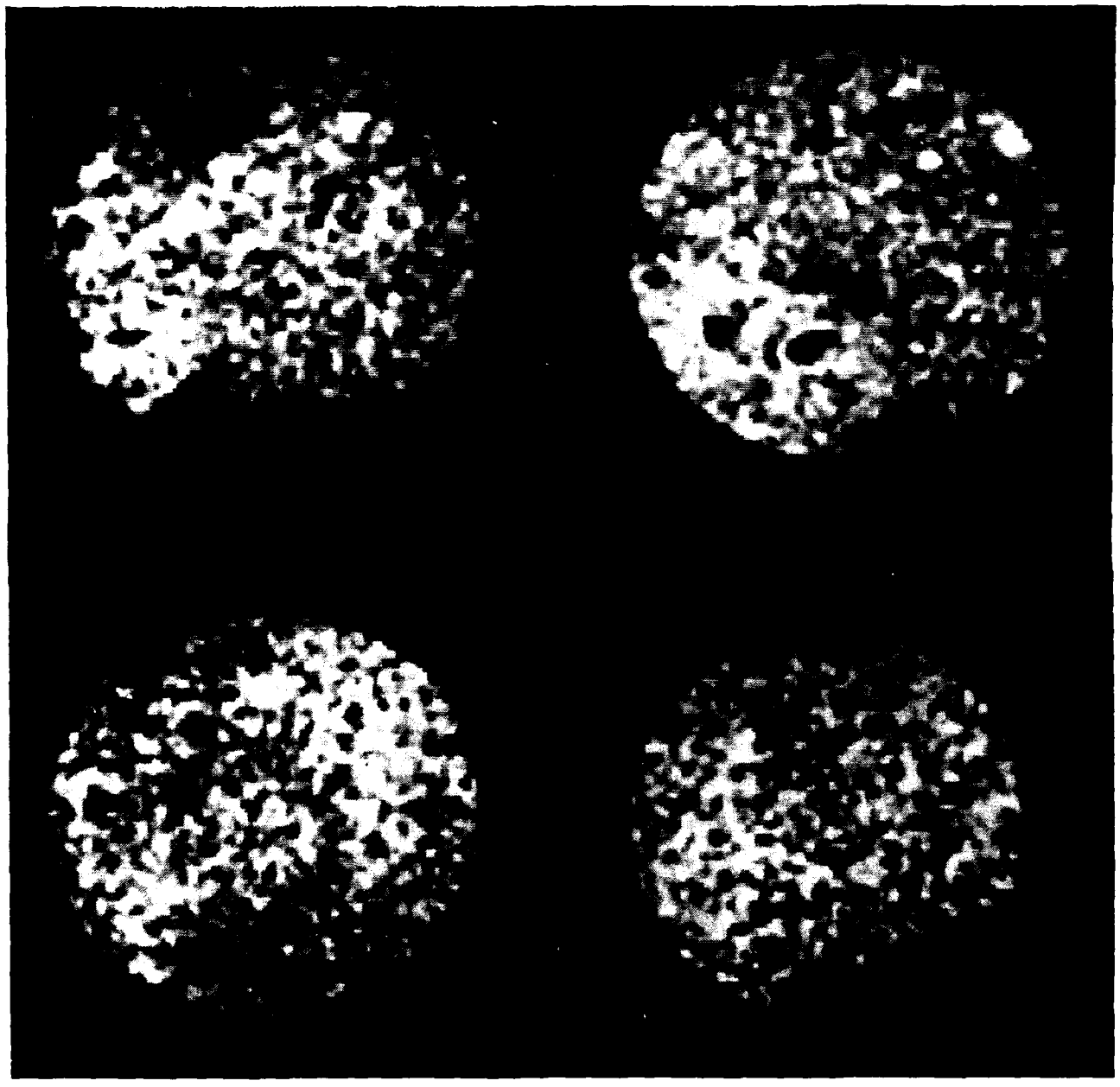

Figure 5: NMR images of H-nuclei in four PBAN simulant samples. Mixing time of samples increases as A → B → C → D.

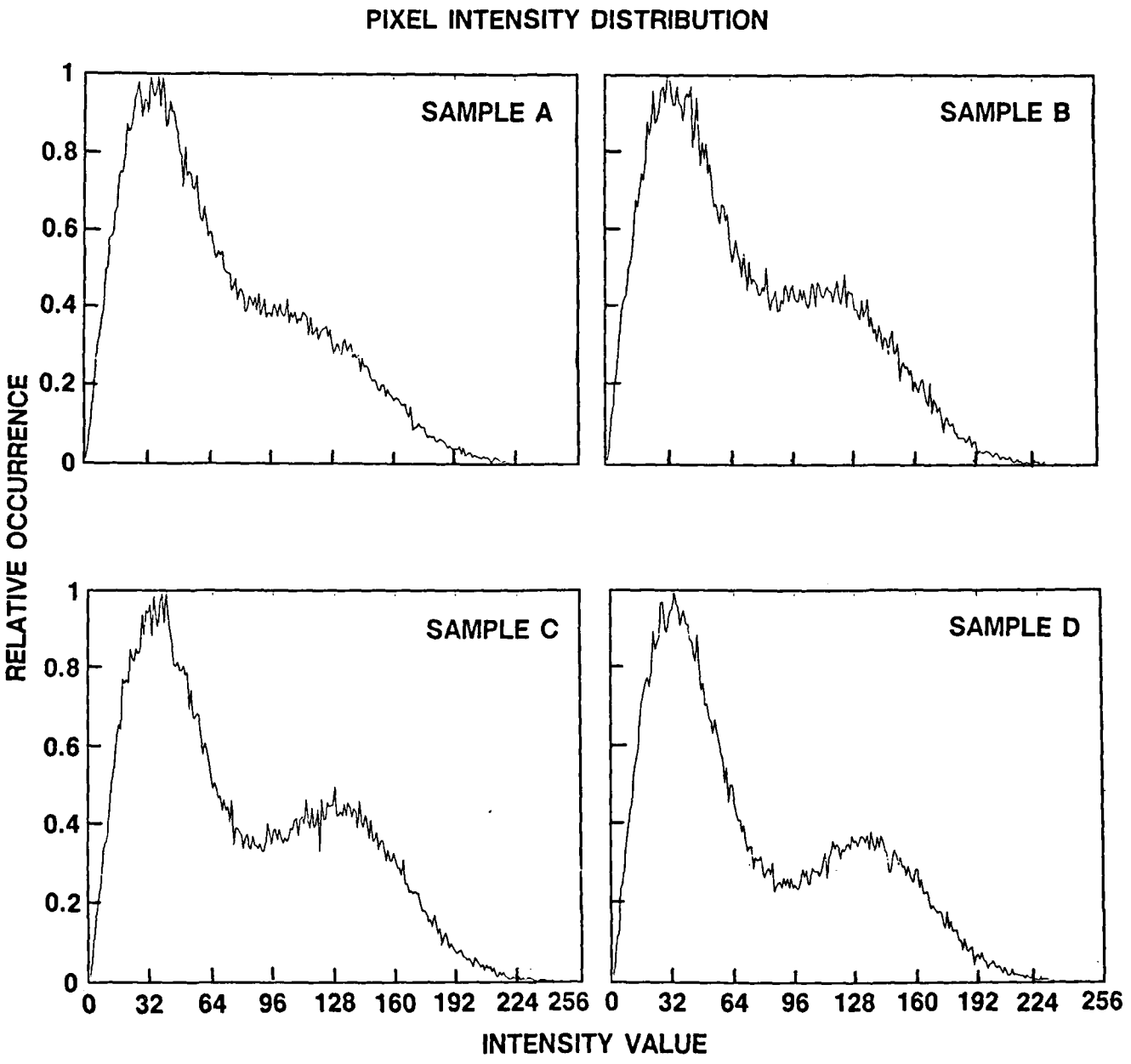


Figure 6: Histogram plots of pixel intensity for each of the four PBAN images (images shown in Figure 5). As mixing time increases (A → B → C → D), separation of signal and noise peaks increases, and width of signal peak decreases.

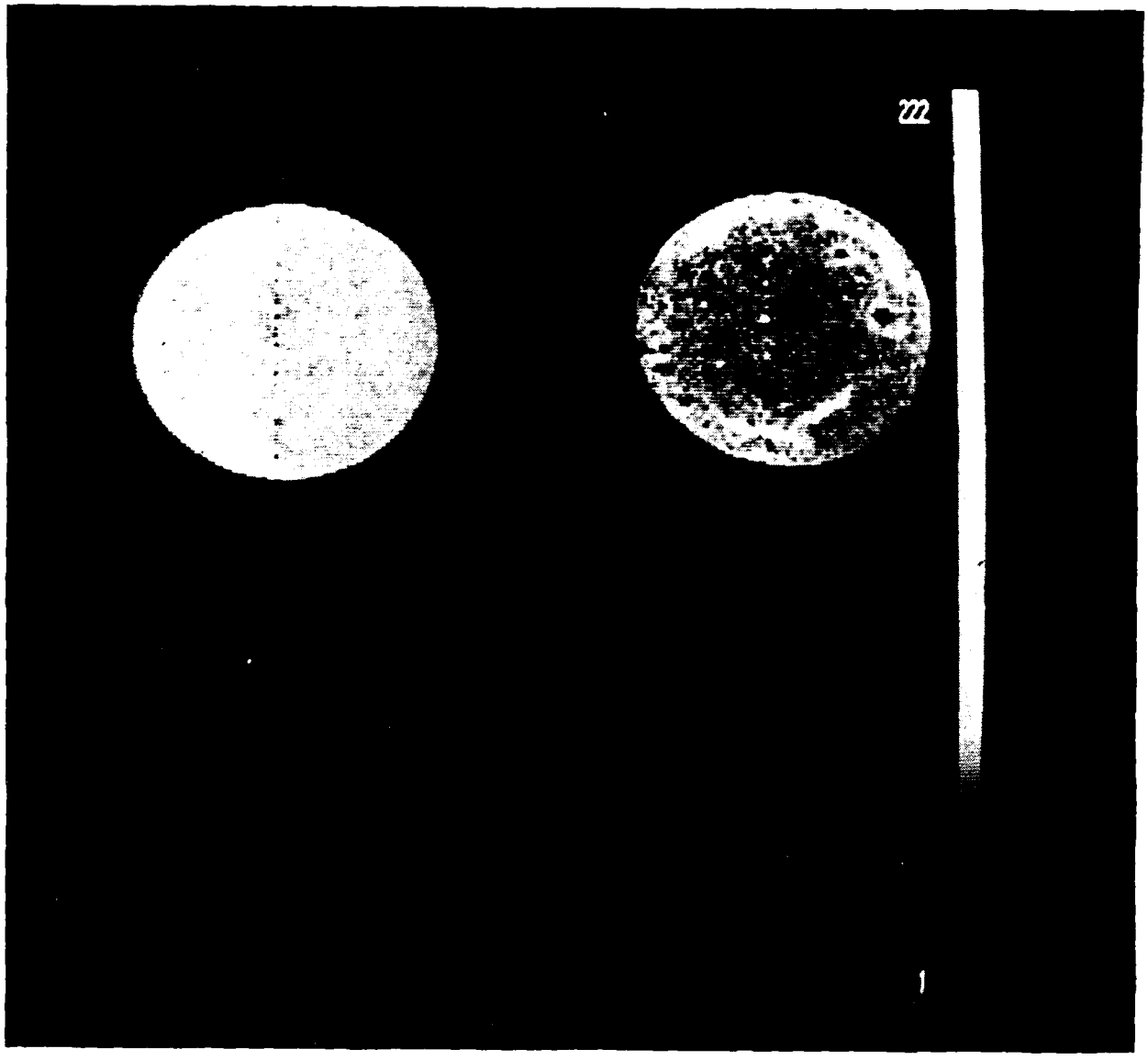

Figure 7: NMR images of hydrogen nuclei in pure glycerine (left) and a suspension of carbon-black in glycerine (right)

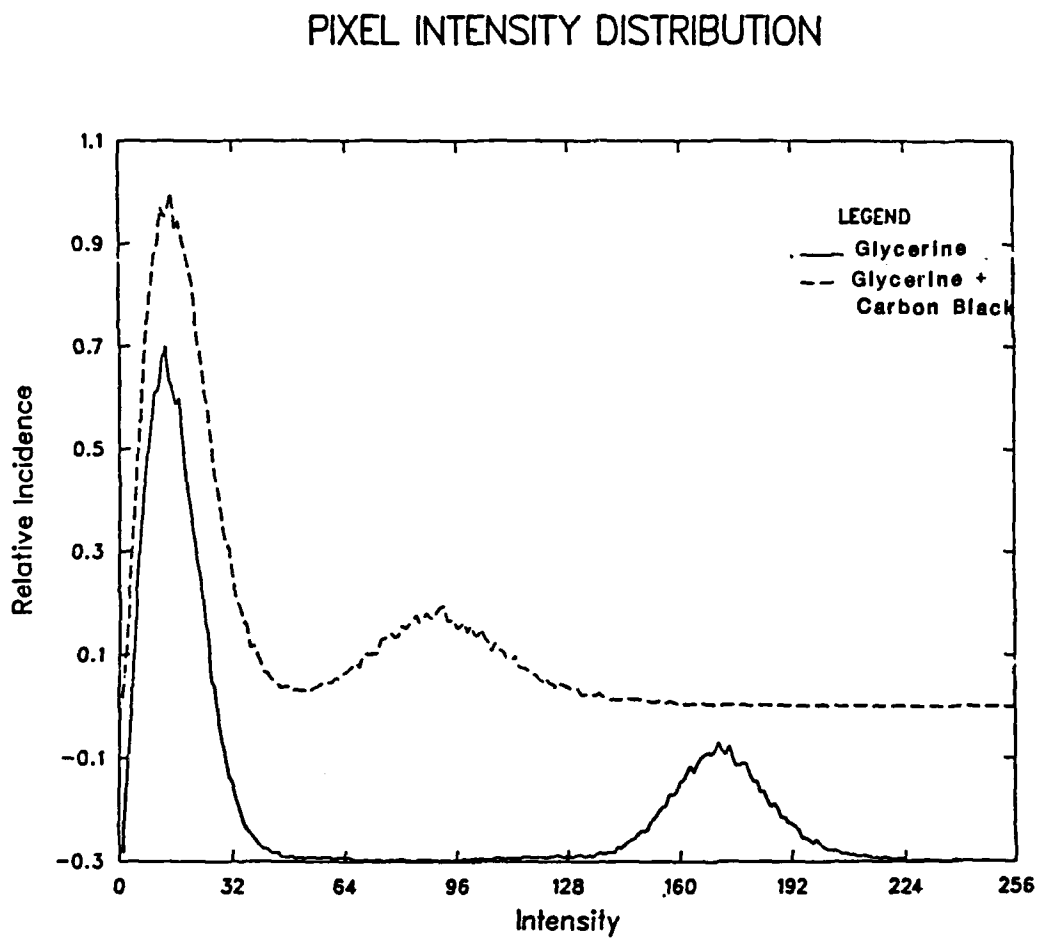


Figure 8: Histogram plots for NMR images of pure glycerine and glycerine/carbon-black suspension (images shown in Figure 7). Histograms have been artificially offset in vertical direction to enhance readability.

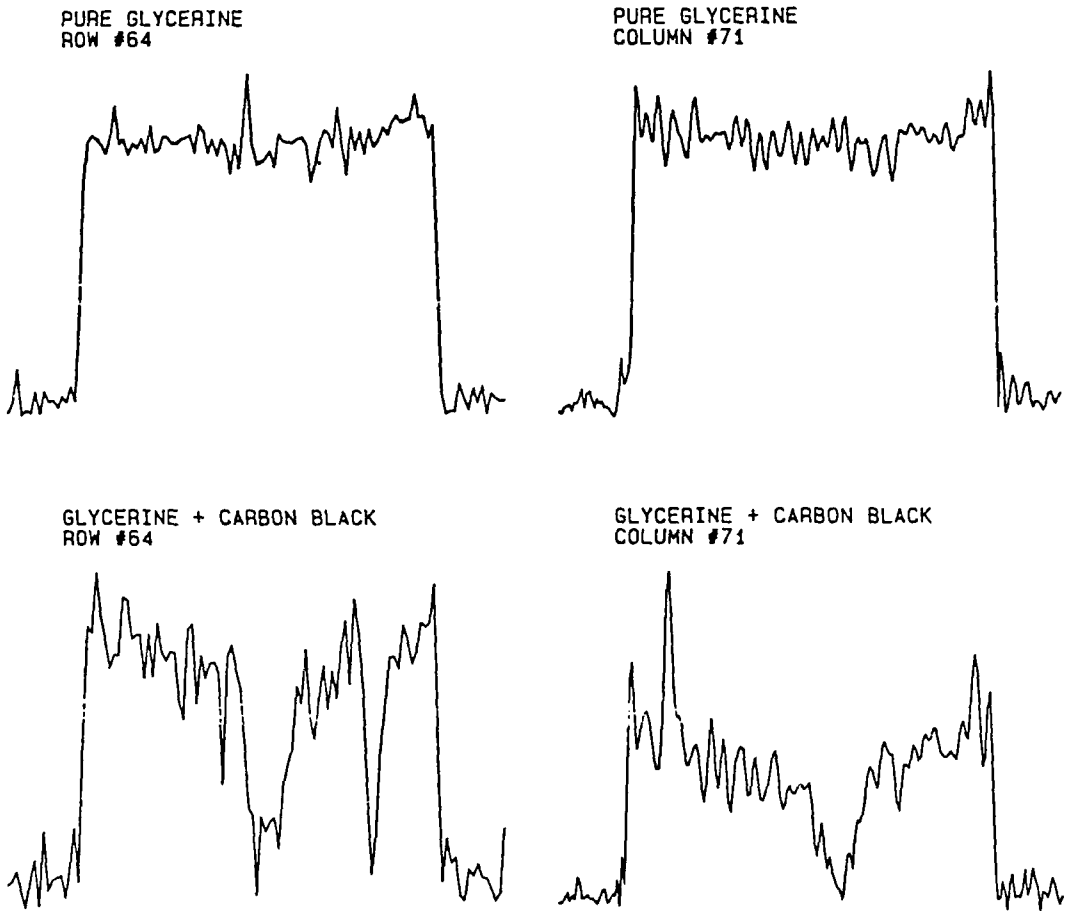


Figure 9: Hydrogen density plot for selected rows and columns in pure glycerine and glycerine / carbon-black NMR images (images shown in Figure 7)

# AUTOCORRELATION FUNCTIONS
# GLYCERINE IMAGES

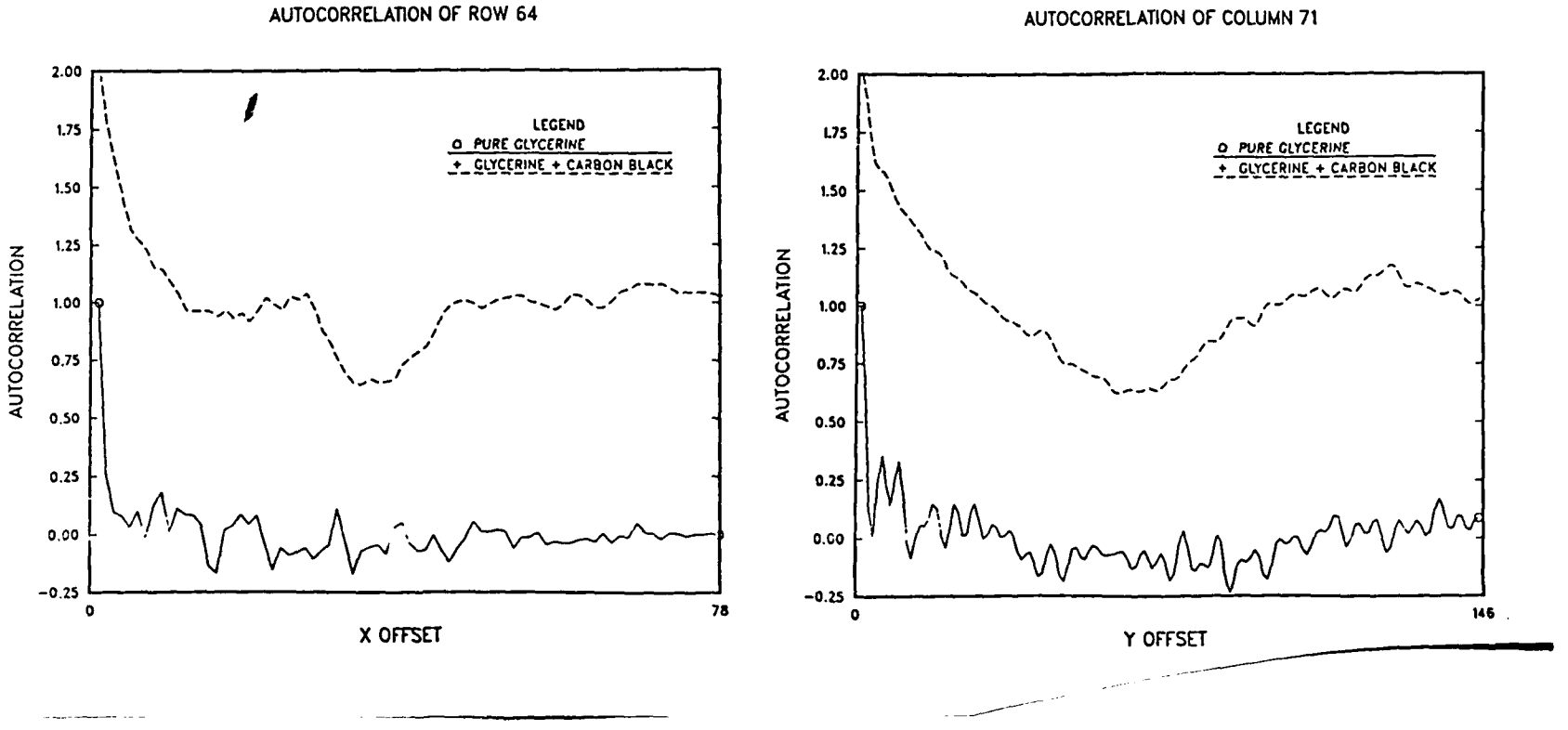


Figure 10: One-dimensional autocorrelation results for selected rows and columns of pure glycerine and glycerine/carbon-black NMR images (images shown in Figure 7)

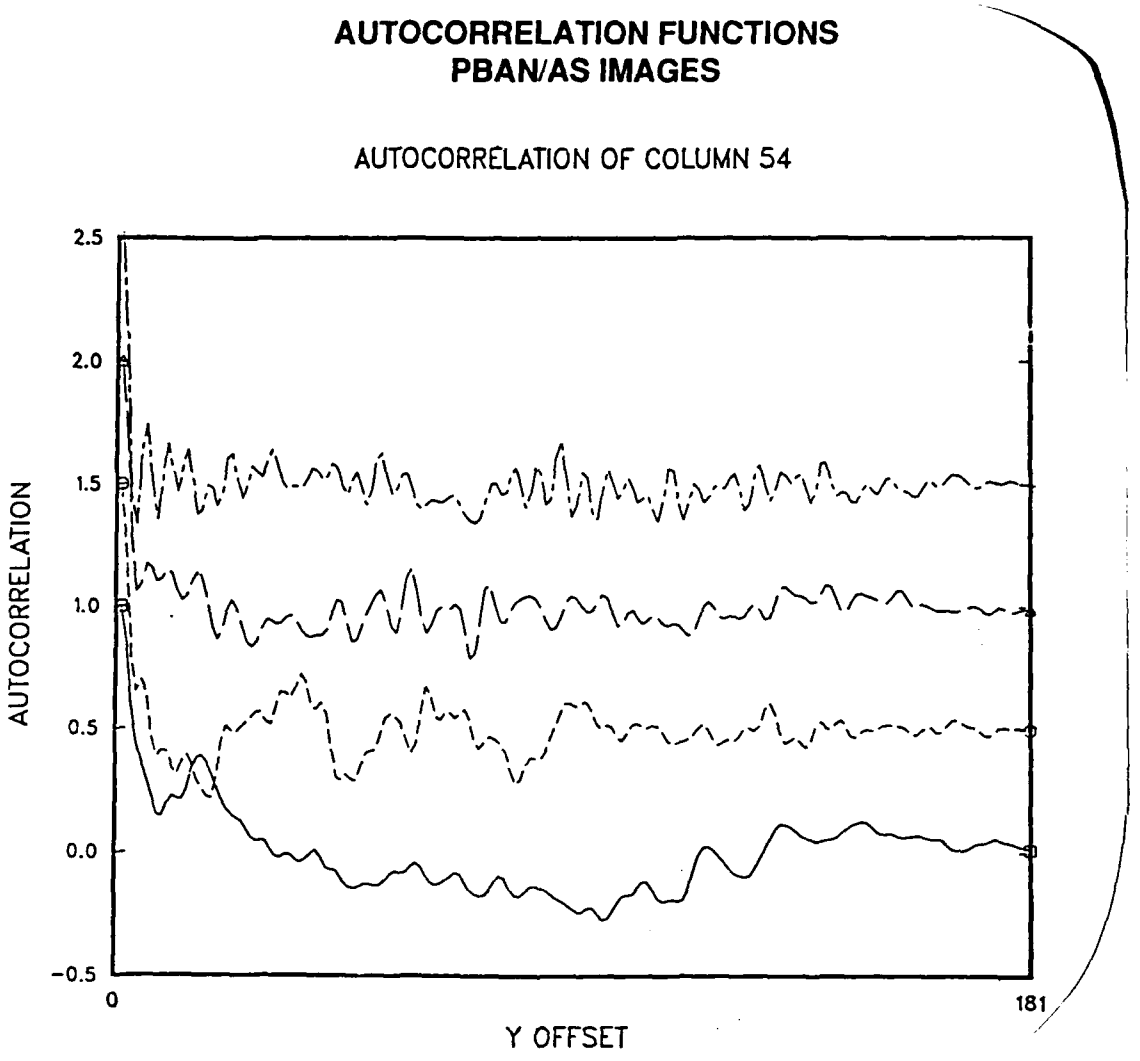


Figure 11: Autocorrelation results for selected columns of PBAN images (images shown in Figure 5)

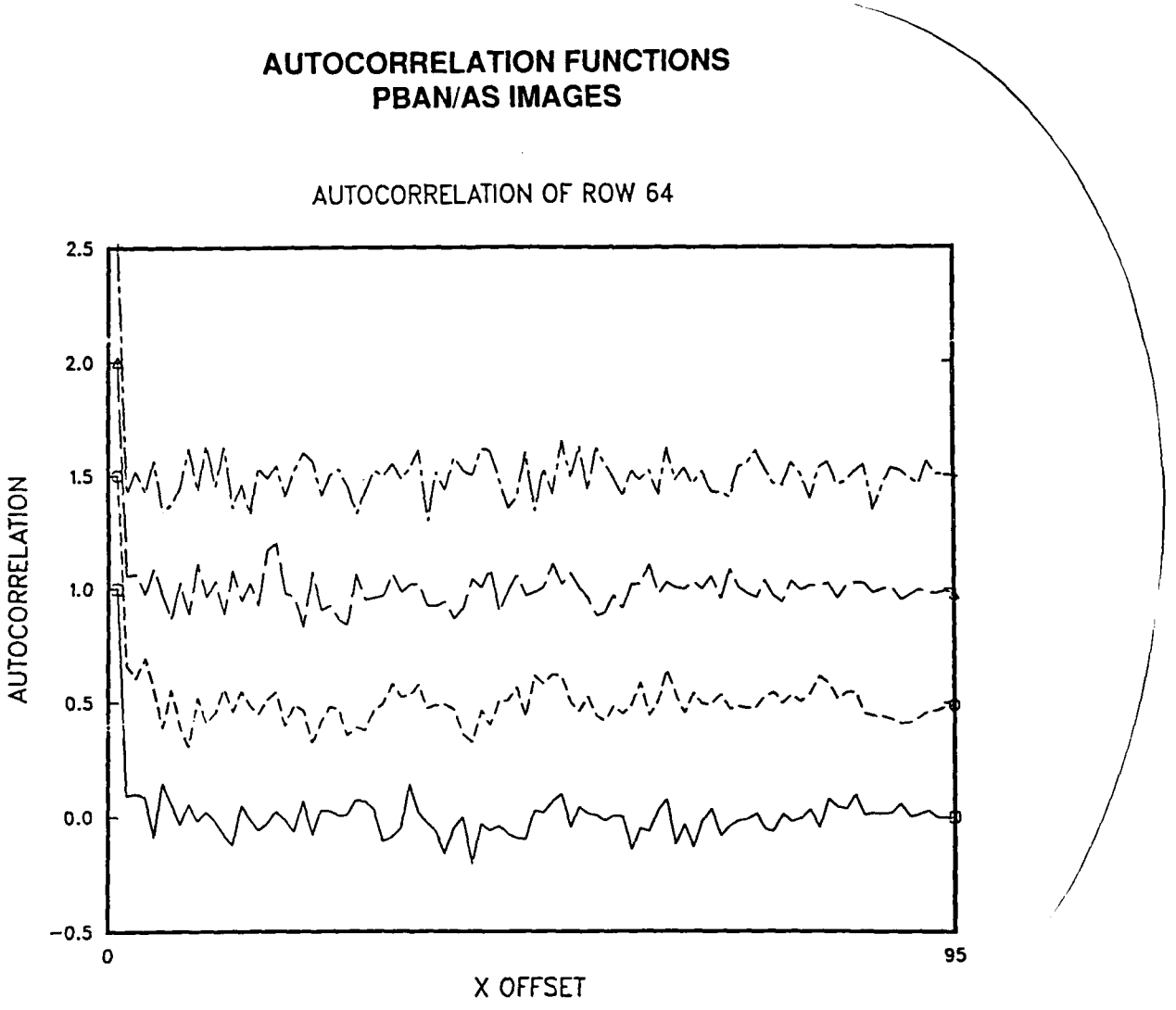


Figure 12: Autocorrelation results for selected rows of PBAN images (images shown in Figure 5)

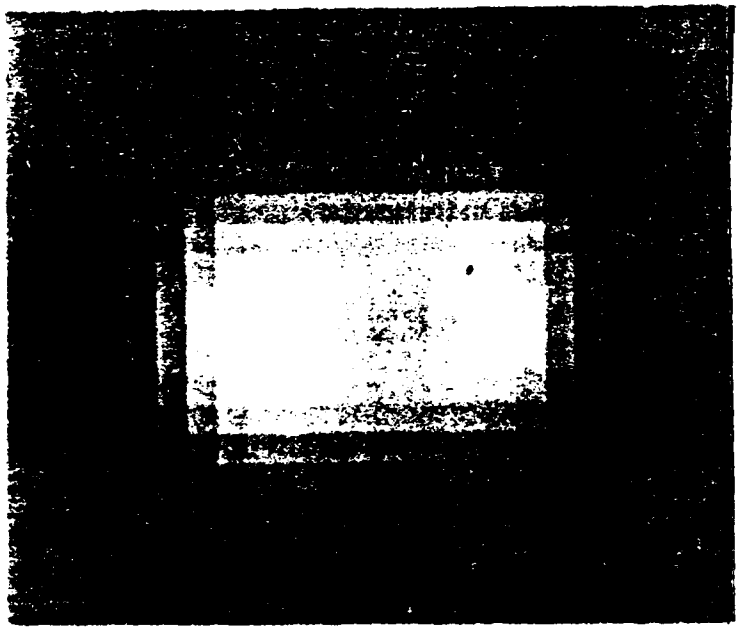

Figure 13: $^{23}Na$ NMR image of PBAN-based propellant simulant sample (15mm x 9mm x 1mm) with hole (9mm x 2.5mm), obtained using initial MTU gradient coil design. Resolution ~3mm.

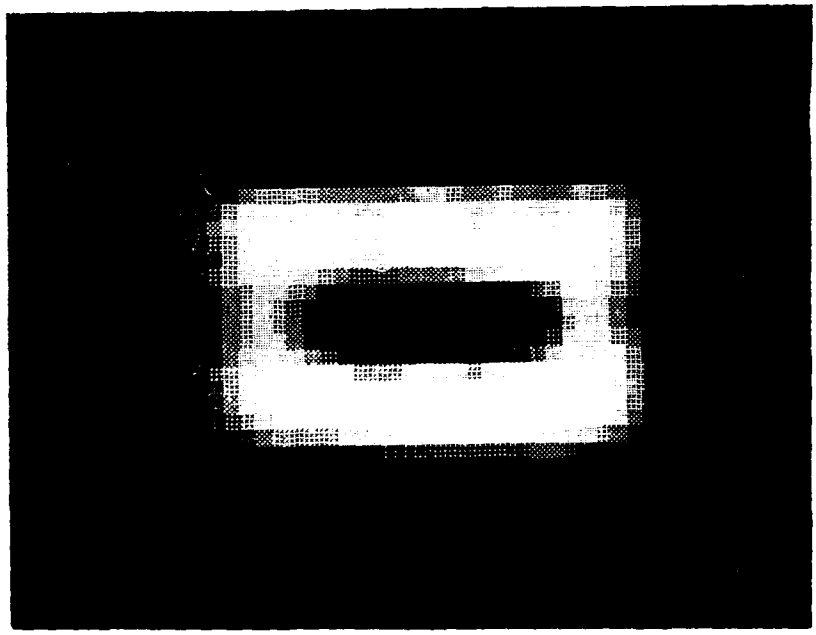

Figure 14: $^{23}Na$ NMR image of PBAN-based propellant simulant sample (15mm x 9mm x 1mm) with hole (9mm x 2.5mm), obtained using improved MTU gradient coil design. Resolution ~1mm.

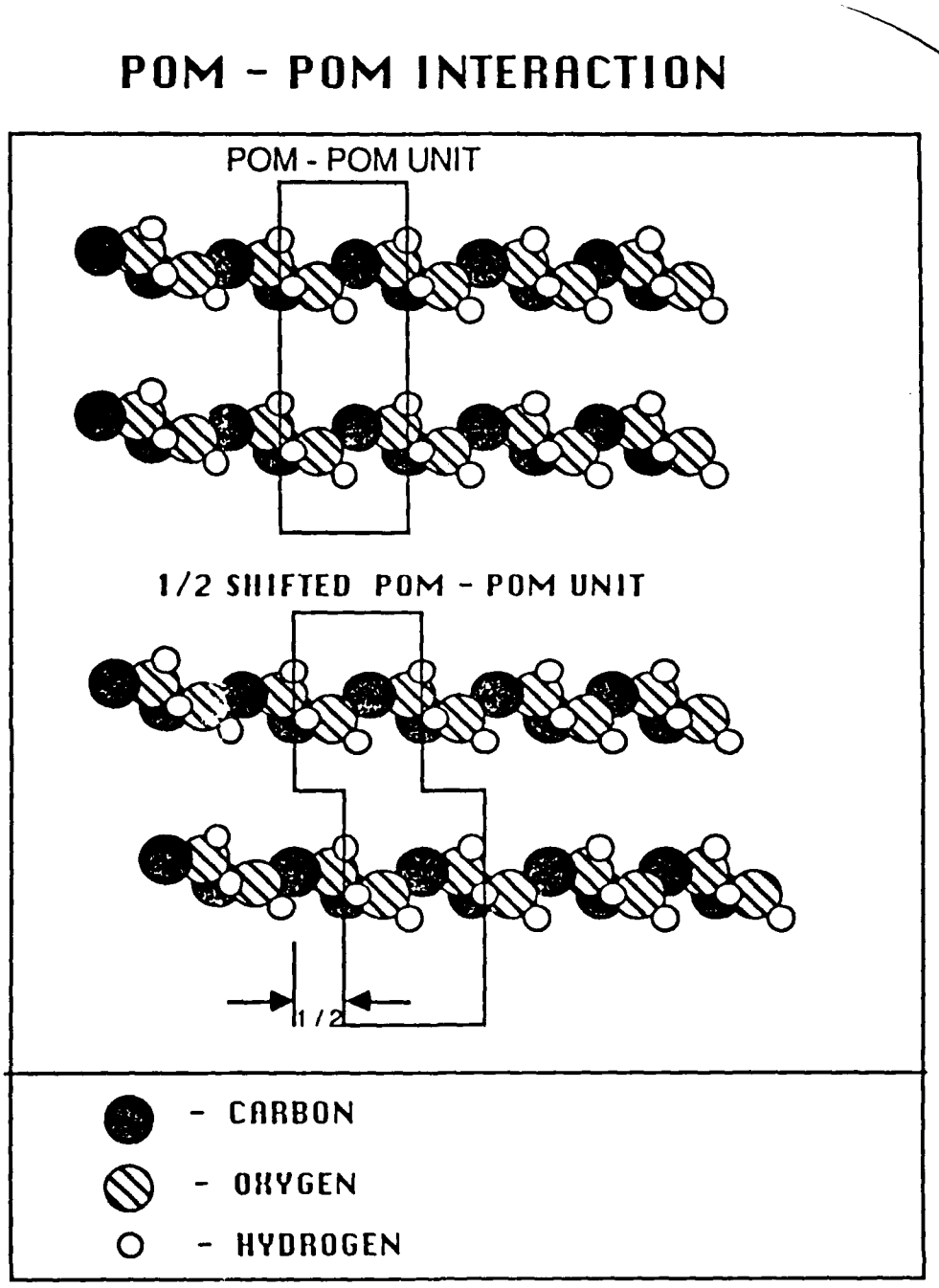


Figure 15: Illustration of Polyoxymethylene-polyoxymethylene interaction

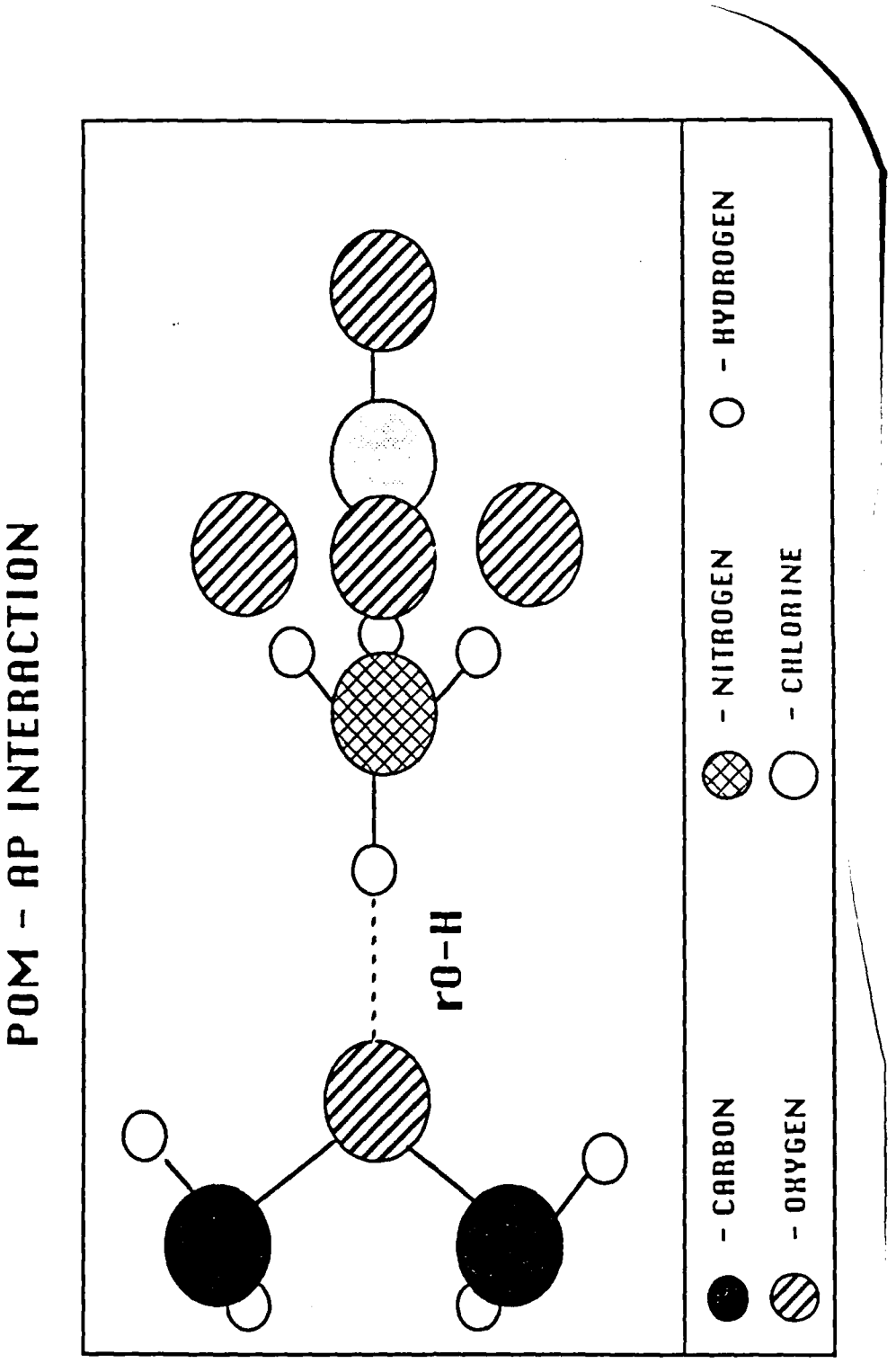


Figure 16: Polyoxymethylene-ammonium perchlorate interaction

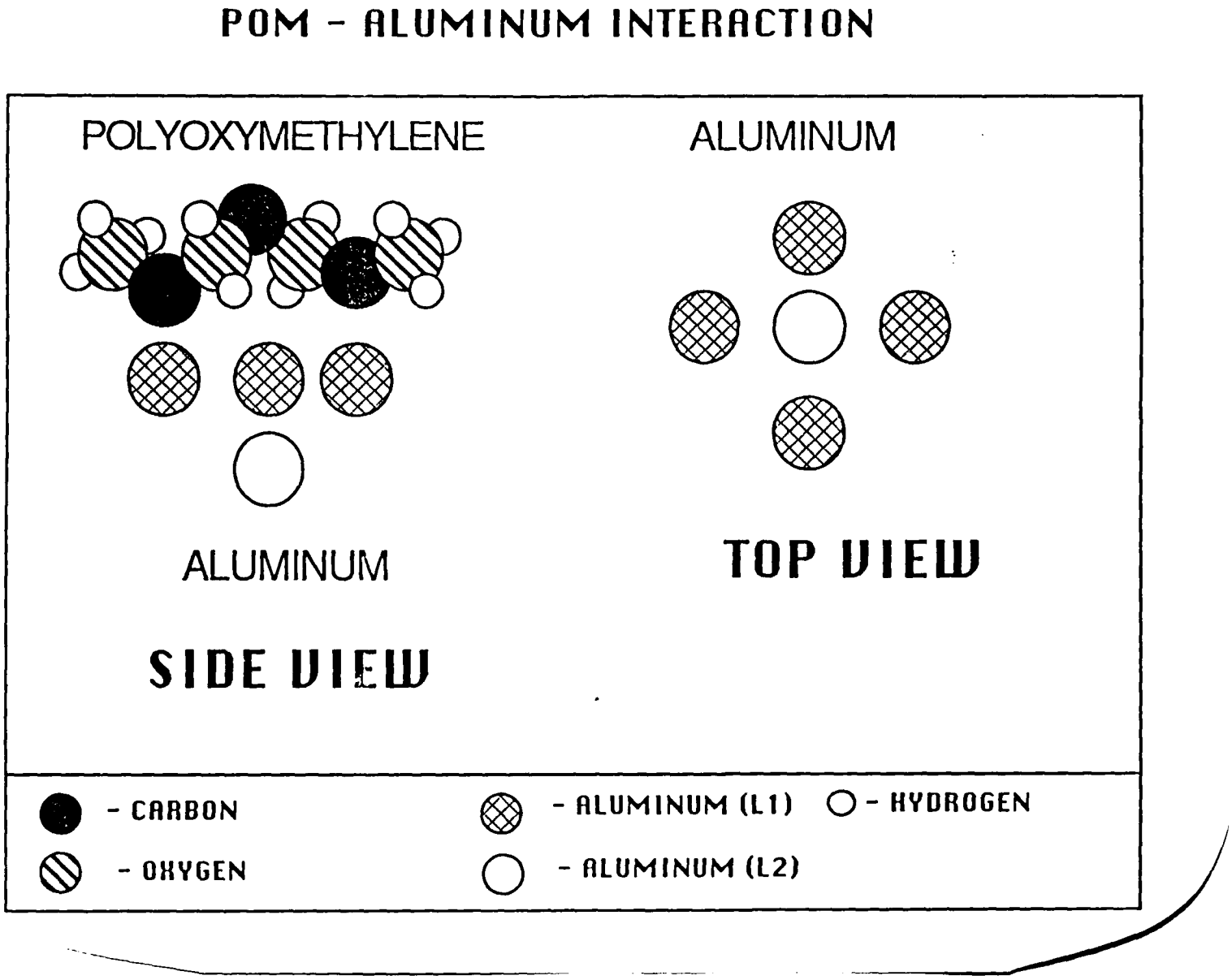


Figure 17: Illustration of Polyoxymethylene-aluminum interaction

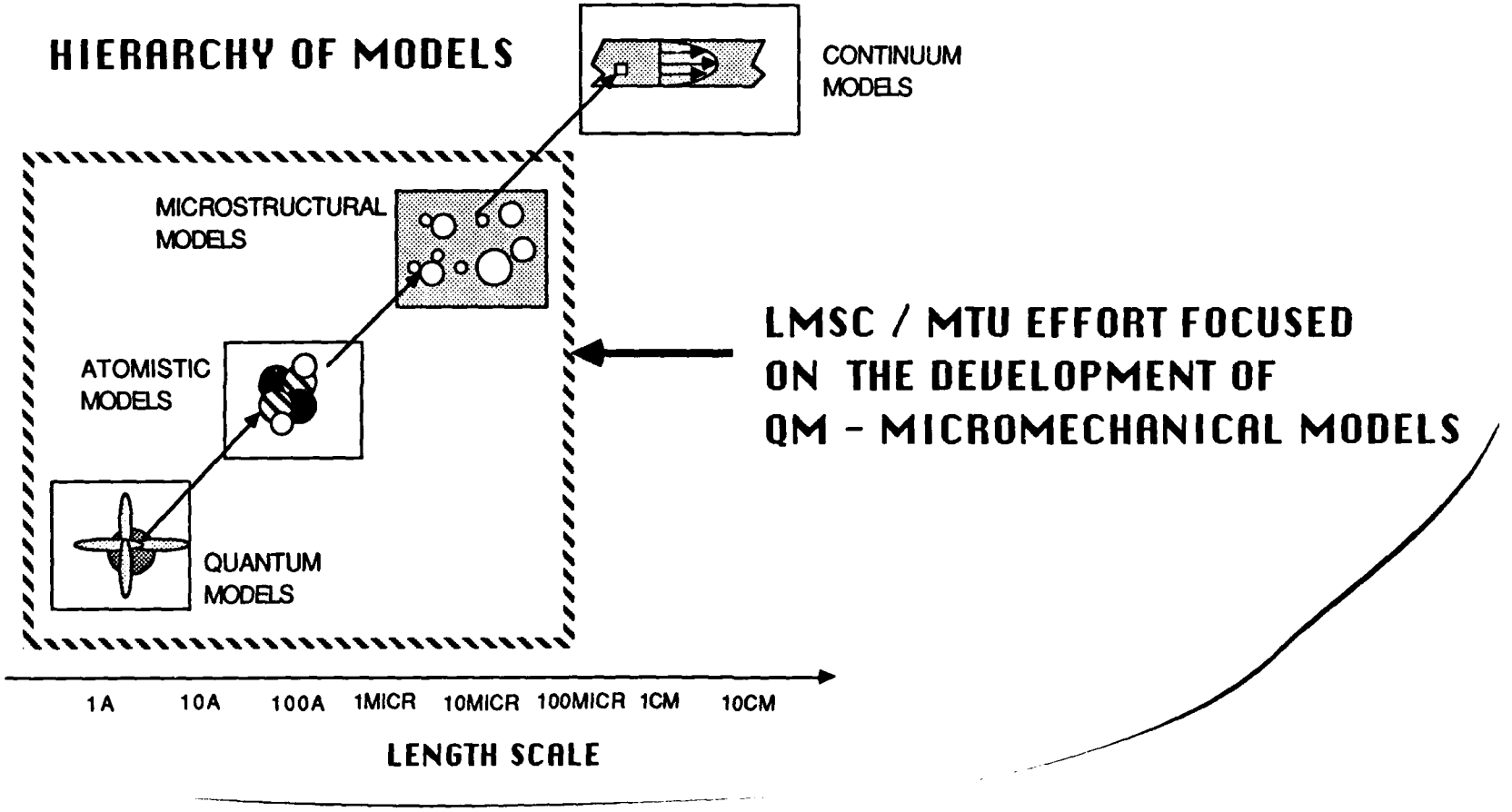


Figure 18: Illustration of model types and length scales

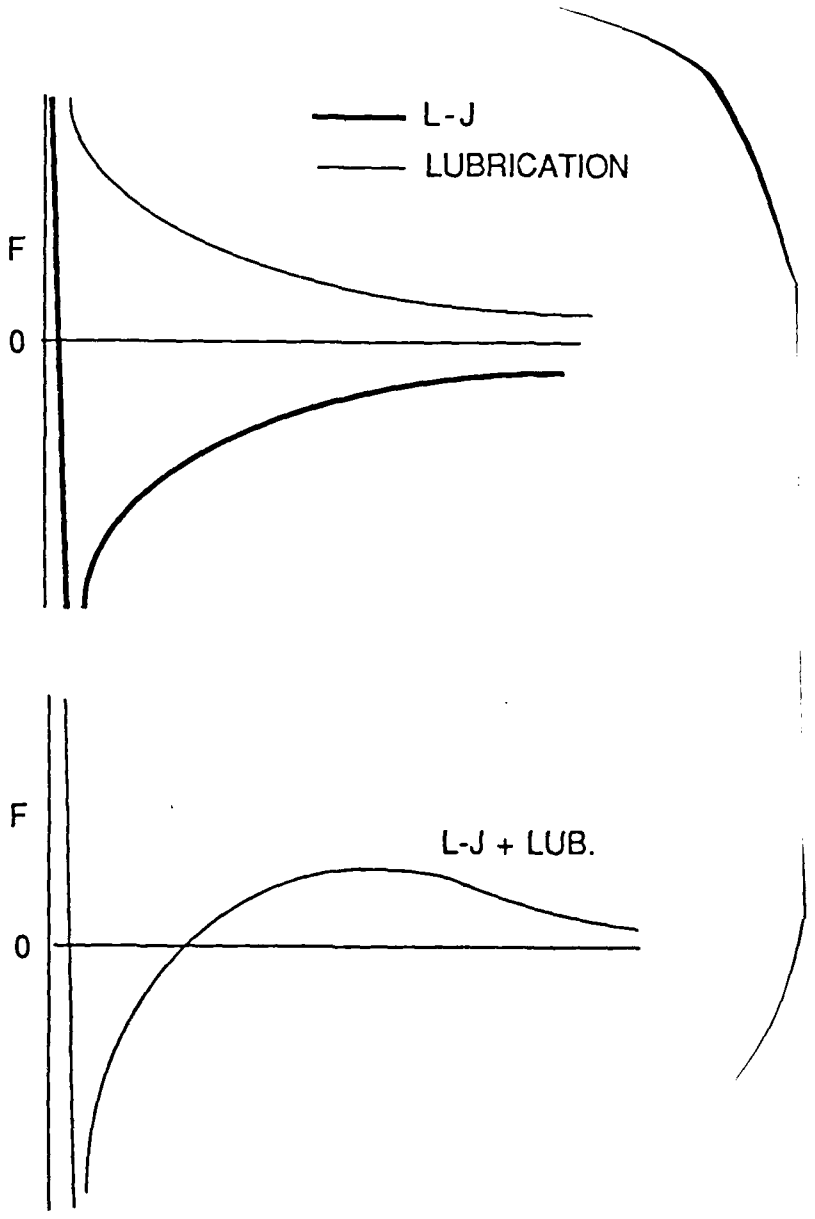


Figure 19: Illustration of Lennard-Jones (L-J) and lubrication *forces as a function* of particle separation distance

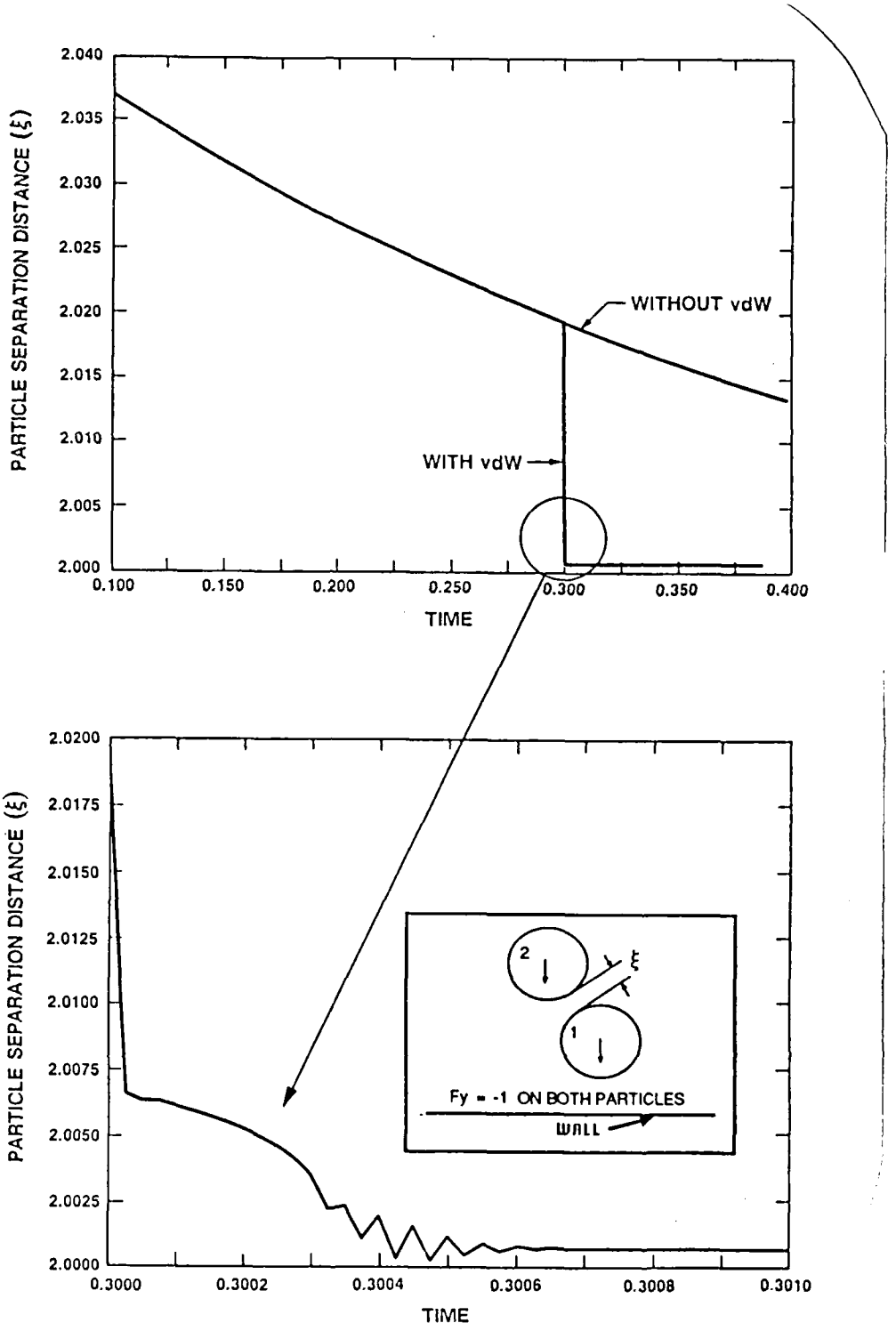


Figure 20: Plots of the inter-particle distance versus time for the two-particle simulation, with and without L-J (van der Waals, or vdW) forces. Basis of the two-particle simulation is illustrated in the figure inset.

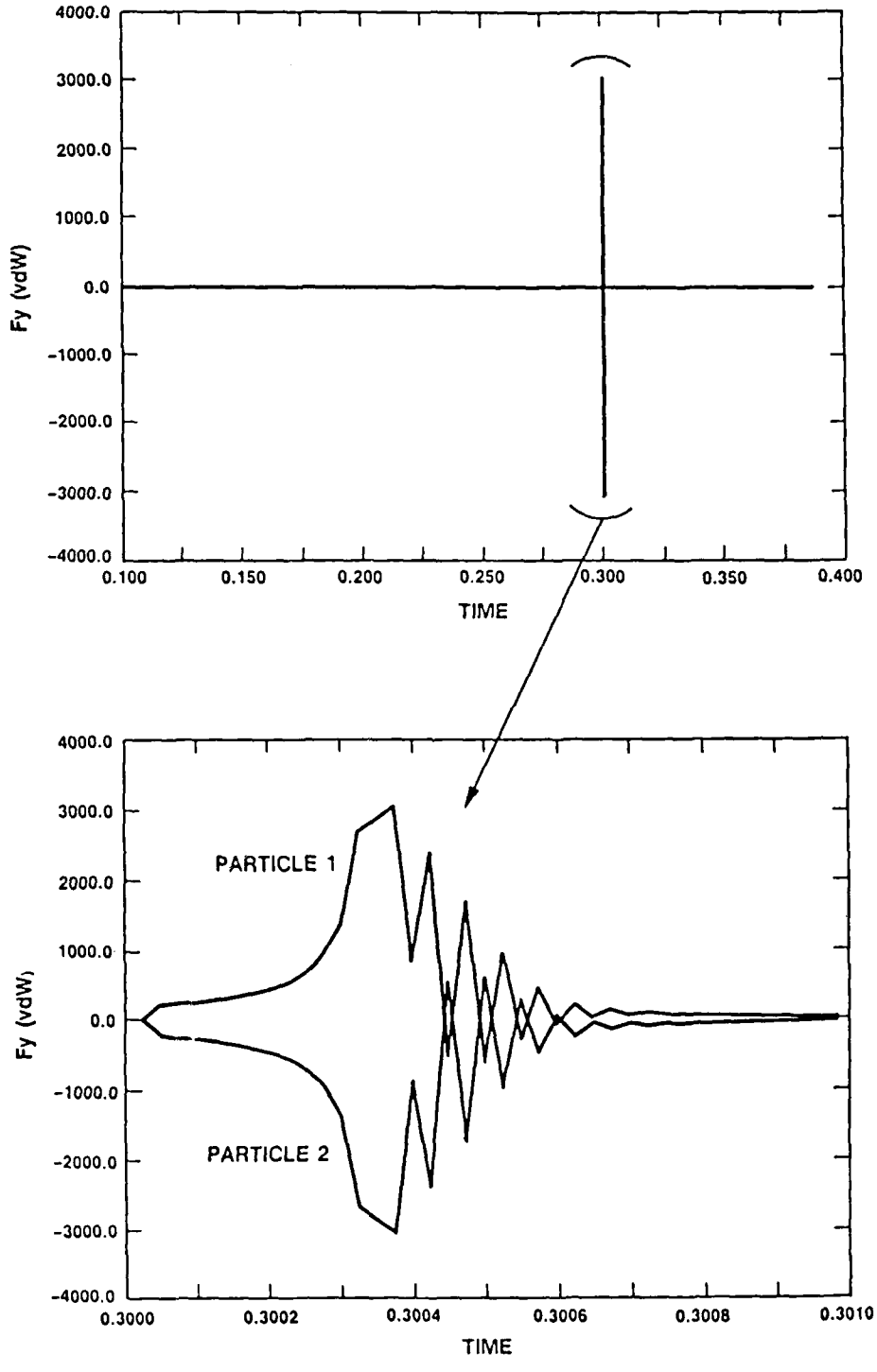


Figure 21: Plots of the relative L-J forces acting on the particles in the two-particle simulation

# ATTACHMENT A

Revised Program Schedule Plan

For 1988 to Early 1989

MAGNETIC RESONANCE STUDIES OF PROCESS RHEOLOGY
Revised Research Schedule for 1988 to early 1989 (3/31/88) (Page 1)

| **EXPERIMENTAL TASKS** | (= 1988 =======)(=1989 |
|---|---|
| **Magnetic Resonance Imaging / Image Processing** | A M J J A S O N D J F M |
| **LPARL Rheological Studies** | |
| Consolidate requests for SIT-supplied samples | Δ---------- |
| Determine rheological analyses to be carried out by SIT and/or LMSC | Δ---------- |
| Rheological analysis | Δ---------- |
| **LPARL NMR** | |
| Stationary Imaging - Homogeneity Study | |
| Define experimental matrix sample requirements | Δ------ |
| NMR Imaging ($\rho$, $T_1$, $T_2$) | Δ---------Δ Δ--- |
| Develop (1) method for determining and (2) mechanism for reporting homog. | Δ----------Δ Δ---- |
| Correlate results to processing parameters (with help from Stevens Inst.) | Δ---Δ Δ--- |
| Flow Imaging | |
| Design / build pilot-scale (2 to 3 inch diameter) flow system | Δ-----Δ Δ--- |
| Refine technique for refocusing flow velocities | Δ------Δ Δ--- |
| Evaluate alternate flow imaging pulse sequences | Δ------Δ Δ--- |
| NMR flow imaging of straight pipe (i.e., images of $\rho$ and velocities) | Δ---- |
| Exotic Imaging Methods - Eval. potential utility and implementation | |
| Multiple Pulse line narrowing and Multiple-Quantum | Δ---------Δ Δ-- |
| **MTU NMR** | |
| Design improved RF coil for imaging applications | Δ------ |
| Build/test imaging probe using improved RF coil design | Δ--- |
| Image Sodium and Aluminum in PBAN simulant using improved imaging probe | Δ--- |
| **MTU ESR** | |
| Determine sample needs, transmit to LMSC | Δ--- |
| Static ESR Imaging | |
| Further evaluate tracers (e.g., MgO, DPPH, TPV) for ESR imaging | Δ---------- |
| Carry out static ESR imaging experiments | Δ---------- |
| ESR Flow Imaging | |
| Design experimental matrix | Δ------ |
| Design & build flow imaging cell | Δ---------- |
| Carry out flow imaging experiments | Δ---------- |

MAGNETIC RESONANCE STUDIES OF PROCESS RHEOLOGY
Revised Research Schedule for 1988 to early 1989 (3/31/88) (Page 2)

| **THEORETICAL MODELING TASKS**<br>**Atomistic, Stokesian Dynamics, Finite Element** | <= 1988 =======>\|<=1989<br>A M J J A S O N D J F M |
|---|---|
| **MTU** | |
| Quantum Mechanics | |
| Evaluate particle-particle and particle-fluid interactions for: | |
| (1) Polyethylene glycol (PEG) - PEG system. Compare to POM-POM. | Δ---------- |
| (2) Polyethylene glycol (PEG) - alumina system. Compare to POM-aluminum. | Δ---------- |
| (3) Determine effect of water on PEG-alumina interactions. | Δ---------- |
| (4) Nitroglycerine - Polyethylene glycol (NG-PEG). | Δ---------- |
| Stokesian Dynamics (SD) | |
| Install SD code | Δ- |
| Develop modified F-ξ relationships for short ranges using QM results for highly loaded POM-alumina suspension system | POM PEG-NG<br>Δ--Δ---------- |
| Implement modified relationships in SD code | Δ--- |
| Finite Element | |
| Investigate availability/capabilities of Flow Dynamics Finite Element codes | Δ-- |
| **LPARL** | |
| Stokesian Dynamics | |
| Provide MTU with basis of existing close range force interactions | Δ-- |
| Provide MTU with order-of-magnitude particle-particle forces | Δ-- |
| Install SD code at MTU | Δ-- |
| Exercise SD code at MTU | Δ---------- |
| Compare 6-particle system behavior with and without vdW interactions | Δ---------- |
| Finite Element (FE) | |
| Investigate availability/capabilities of Flow Dynamics (FD) FE codes | Δ-- |
| Exercise FD code for NMR/ESR flow probe geometries, if needed | Δ- |